ELSEVIER

Cancer Genetics and Cytogenetics 188 (2009) 99–102

Cancer Genetics and Cytogenetics

Short communication

# Transient abnormal myelopoiesis in a Down syndrome newborn followed by acute myeloid leukemia: identification of the same chromosomal abnormality in both stages

Toshiyuki Kitoh[a,b,*], Tomohiko Taki[c], Yasuhide Hayashi[d], Kenji Nakamura[e], Tamotsu Irino[b,f], Mitsuhiko Osaka[f]

[a]*Department of Hematology/Oncology, Shiga Medical Center for Children, 5-7-30 Moriyama, Moriyama 524-0022, Moriyama, Japan*
[b]*Department of Laboratory Medicine, Shiga Medical Center for Children, Moriyama, Japan*
[c]*Department of Molecular Laboratory Medicine, Kyoto Prefectural University of Medicine Graduate School of Medical Science, Kyoto, Japan*
[d]*Gunma Children's Medical Center, Gunma, Japan*
[e]*Department of Pediatrics, Otsu Red Cross Hospital, Otsu, Japan*
[f]*Division of Cancer Research, Shiga Medical Center Research Institute. Moriyama, Japan*

Received 18 June 2008; received in revised form 31 July 2008; accepted 13 August 2008

**Abstract** A transient abnormal myelopoiesis was observed in a newborn with Down syndrome. Cytogenetic study revealed multiple oligoclonal abnormalities: 47,XY,inv(6)(p23q21),+21c[3]/47,XY, der(7)t(1;7)(q25;p15),+21c[1]/47,XY,del(13)(q?),+21c[1]/47,XY,+21c[15]. Ten months after the patient achieved remission, the transient abnormal myelopoiesis evolved to an acute megakaryoblastic leukemia. Cytogenetic study revealed only a single clonal abnormality, 47,XY,der(7)t(1;7)(q25;p15),+21c, identical to one of the structural changes seen at birth. Sequence analysis of the *GATA1* gene revealed a deletion–insertion mutation within the exon 2 introducing a stop codon after Arg 64. It may be that the der(7)t(1;7)(q25;p15) abnormality played some selective role in the development of acute megakaryoblastic leukemia in this patient. To our knowledge, the present case is unique in demonstrating a subclone with der(7)t(1;7)(q25;p15) evolving to acute leukemia. 

## 1. Introduction

Approximately 10% of patients with Down syndrome are born with transient abnormal myelopoiesis (TAM) [1,2]. Of these cases, ~20% recur as acute megakaryoblastic leukemia (AMKL) [3]. Acquired mutations in *GATA1* in the leukemic blasts are detected in virtually all of these cases [4–7], but the second hit for the full expression of AMKL is still a matter of discussion [6,7]. GATA1 is a transcription factor that regulates megakaryocytic differentiation, and the mutations observed are considered to cause accumulation of poorly differentiated megakaryocytic precursors [4]. Strikingly, *GATA1* is located on chromosome X; therefore, genetic interaction of *GATA1* with one or more genes on other chromosomes presumably contributes to the development of AMKL in Down syndrome.

Acute myeloid leukemia (AML) and myelodysplastic syndrome (MDS) in Down syndrome often demonstrate chromosomal abnormalities in addition to the constitutional trisomy 21 [8–12]. These include both numerical and structural abnormalities, mostly complete or partial trisomy of a specific chromosome; reciprocal translocations are relatively rare. The role of these chromosomal translocations in developing leukemia in Down syndrome is also unknown. Here, we report the case of a Down syndrome patient who developed AMKL showing der(7)t(1;7)(q25;p15) following TAM at birth.

## 2. Case report

This Down syndrome patient was a boy born at 39 weeks gestational age, weighing 3,235 g. Thrombocytopenia was revealed after birth. At 5 days after birth, he was diagnosed as having TAM. Initial white blood cell count was 13,200/μL with 7% blasts, hemoglobin was 15.0 g/dL, and platelet count was 52,000/μL. Chromosomal analysis of bone marrow cells at diagnosis revealed the

* Corresponding author. Tel.: +81-77-582-6200; fax: +81-77-582-6304. (T. Kitoh).
*E-mail address:* tkitoh-mccs@umin.ac.jp (T. Kitoh).

0165-4608/09/$ – see front matter 
doi:10.1016/j.cancergencyto.2008.08.011

Fig. 1. Karyogram of the blast in leukemic phase showing 47,XY,der(7)t(1;7)(q25;p15),+21c.

karyotype 47,XY,inv(6)(p23q21),+21c[3]/47,XY,der(7)t(1;7)(q25;p15),+21c[1]/47,XY,del(13)(q?),+21c[1]/47,XY,+21c[15]/. Although he was not treated, his white blood cell count gradually decreased within 2 months, and at 7 months after birth his platelet count spontaneously recovered to within the normal range (although he suffered from thrombocytopenia due to an unknown viral infection). At 10 months after birth, the blasts increased suddenly.

Persistent thrombocytopenia was noted after platelet transfusions twice weekly. A bone marrow aspirate showed excessive myelofibrosis. Immunophenotyping of peripheral blasts showed $CD7^+$, $CD13^+$, $CD33^+$, $CD38^+$, $CD41^+$, $CD42b^+$, $CD56^+$, $CD157^+$, and HLA-$DR^+$. Chromosome analysis showed a der(7)t(1;7)(q25;p15) abnormality, in addition to the constitutional trisomy 21 (Fig. 1). Spectral karyotyping further confirmed the presence of the t(1;7) translocation, expressed as 47,XY,der(7)t(1;7)(q25;p15),+21c (Fig. 2), resulting in partial trisomy of 1q.

We analyzed the *GATA1* mutation in the peripheral blood sample, after written informed consent was obtained from his parents. Genomic DNA was extracted, and then polymerase chain reaction (PCR) was performed. Subcloning and nucleotide sequencing of PCR products were performed as described previously [6]. Sequence analysis of *GATA1* gene revealed a deletion–insertion mutation within exon 2, introducing premature stop codon after Arg 64 (Fig. 3).

A trephine biopsy revealed the presence of a typical megakaryocyte proliferation and prominent fibrosis. The final diagnosis of AMKL led to the initiation of combination therapy of pirarubicin HCl (25 mg/$m^2$ per day for 2 days), cytosine arabinoside (100 mg/$m^2$ per day for 7 days), and etoposide (150 mg/$m^2$ per day for 3 days) [13]. Complete remission was achieved after two courses of the therapy. Continuation of the consolidation therapy was uneventful, and six cycles of the same regimen were completed. As of writing, the patient had been in continuous complete remission without marked side effects for 5 years after initiation of the therapy.

## 3. Discussion

Recent collaborative studies on AML in Down syndrome children have established that the most frequent cytogenetic abnormality in AML or MDS in Down syndrome is trisomy 8 or partial trisomy of 1q [2,14–17]. Because AML and MDS with Down syndrome have distinct biologic and clinical features, the identification of Down syndrome patients with a mild or normal phenotype in the AML/MDS population is of fundamental importance for clinical diagnosis and management. Partial trisomy of 1q

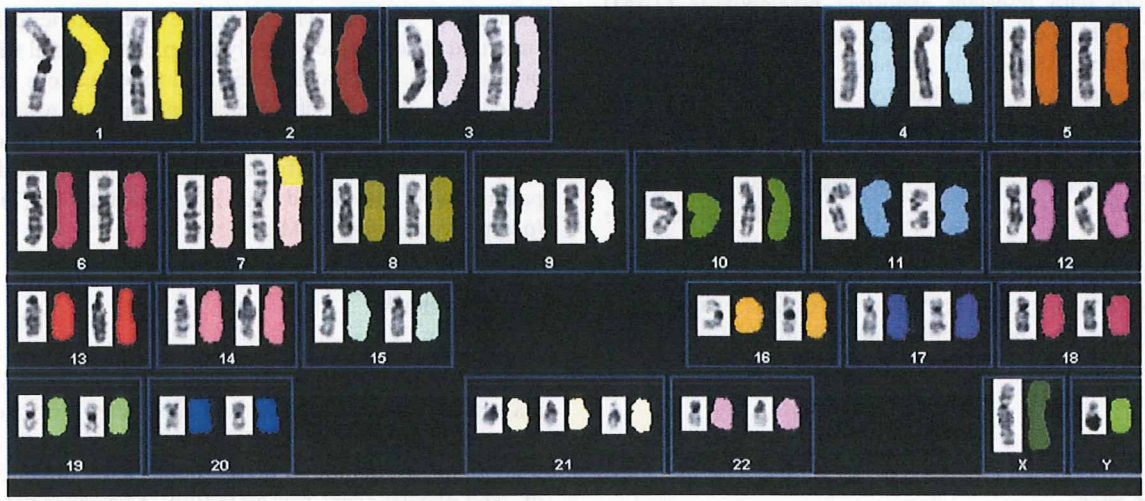


Fig. 2. Spectral karyotyping showing 47,XY,der(7)t(1;7)(q25;p15),+21c.

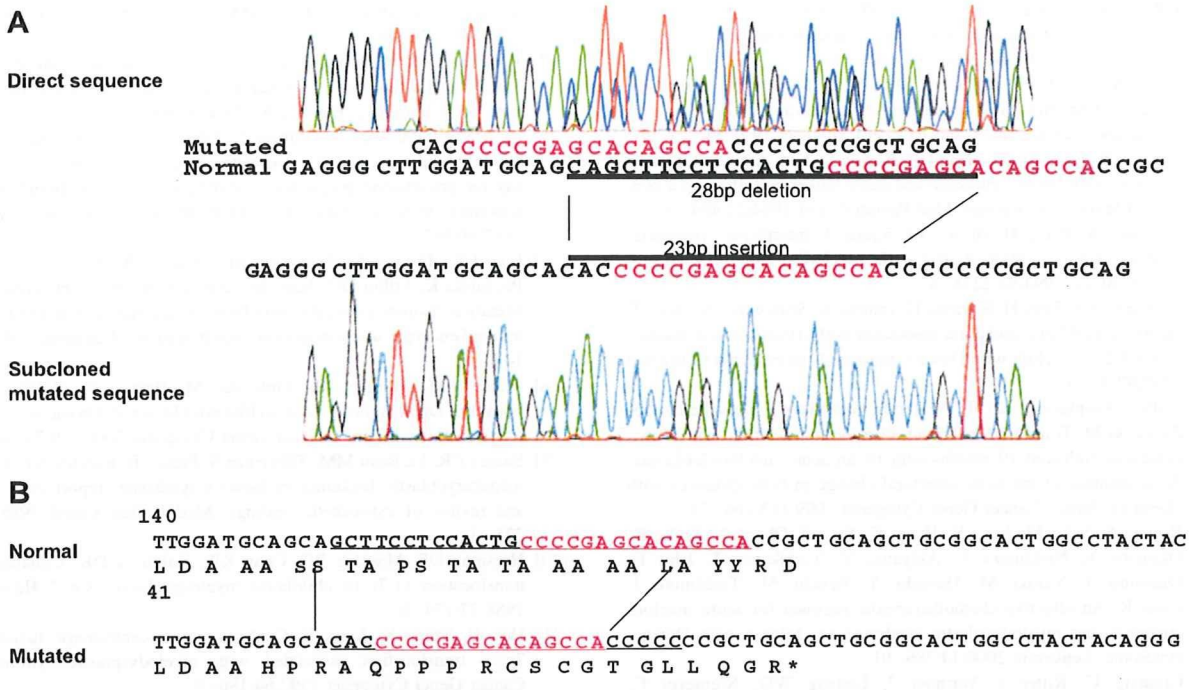


Fig. 3. Mutational analysis of the *GATA1* gene. (A) Sequence analysis was performed directly and using subcloned polymerase chain reaction product and showed a deletion–insertion mutation (28-bp deletion and 23-bp insertion) between 152 and 179 within exon 2. (B) This deletion–insertion mutation introduced a premature stop codon after Arg64. Numbers represent nucleotides from the 5′ end of exon 2.

has been reported by several authors and appears to represent a nonrandom chromosomal abnormality in patients with MDS/AML and Down syndrome [14,17]. Partial trisomy of 7q [8] or monosomy 1 [18,19] have also been reported. Unbalanced translocation t(1;7) in childhood myelodysplasia has been reported [20]. It is also possible that the t(1;7) played some role in the development of the MDS [21]. The mechanism of formation of the der(7)t(1;7) and its role in leukemogenesis are still unclear. Given that der(7)t(1;7) results in partial trisomy of 1q and partial monosomy of 7q, the increased dosage of the oncogenes located at 1q or the loss of the tumor suppressor genes located at 7q (or both factors) may be implicated in leukemogenesis of MDS and AML with der(7)t(1;7).

Cases of TAM usually have no karyotypic abnormality [1], but AMKL is associated with chromosomal abnormalities, including 8 trisomy and 19 trisomy [2]. Rare TAM cases have had chromosome abnormalities that were also observed in developing AMKL [22]. As for the *GATA1* gene, the deletion–insertion mutations within exon 2 in our patient have been reported previously in only two cases of TAM [5,7]. Reciprocal translocations are rare in TAM with Down syndrome. In the present case, a der(7)t(1;7) with partial trisomy of 1q, which is among the most frequently observed abnormalities in Down syndrome, might contribute to evolution to acute leukemia. The present report contributes insight into the mechanism of leukemic transformation from TAM in Down syndrome.

## Acknowledgments

This work was supported by a grant-in-aid for cancer research from the Ministry of Health, Labor, and Welfare of Japan.

## References

[1] Hayashi Y, Hanada R, Yamamoto K, Ohde S, Niitsu N, Eguchi M, Sugita K, Nakazawa S. Transient megakaryoblastic proliferation in a newborn infant with Down's syndrome. Cancer Genet Cytogenet 1987;28:373–4.

[2] Hayashi Y, Eguchi M, Sugita K, Nakazawa S, Sato T, Kojima S, Bessho F, Konishi S, Inaba T, Hanada R. Cytogenetic findings and clinical features in acute leukemia and transient myeloproliferative disorder in Down's syndrome. Blood 1988;72:15–23.

[3] Hitzler JK, Zipursky A. Origins of leukaemia in children with Down syndrome. Nat Rev Cancer 2005;5:11–20.

[4] Wechsler J, Greene M, McDevitt MA, Anastasi J, Karp JE, Le Beau MM, Crispino JD. Acquired mutations in *GATA1* in the megakaryoblastic leukemia of Down syndrome. Nat Genet 2002;32:148–52.

[5] Rainis L, Bercovich D, Strehl S, Teigler-Schlegel A, Stark B, Trka J, Amariglio N, Biondi A, Muler I, Rechavi G, Kempski H, Haas OA, Izraeli S. Mutations in exon 2 of *GATA1* are early events in megakaryocytic malignancies associated with trisomy 21. Blood 2003;102:981–6.

[6] Xu G, Nagano M, Kanezaki R, Toki T, Hayashi Y, Taketani T, Taki T, Mitui T, Koike K, Kato K, Imaizumi M, Sekine I, Ikeda Y, Hanada R, Sako M, Kudo K, Kojima S, Ohneda O, Yamamoto M, Ito E. Frequent mutations in the *GATA-1* gene in the transient myeloproliferative disorder of Down syndrome. Blood 2003;102:2960–8.

[7] Hitzler JK, Cheung J, Li Y, Scherer SW, Zipursky A. *GATA1* mutations in transient leukemia and acute megakaryoblastic leukemia of Down syndrome. Blood 2003;101:4301–4.

[8] Bunin N, Nowell PC, Belasco J, Shah N, Willoughby M, Farber PA, Lange B. Chromosome 7 abnormalities in children with Down syndrome and preleukemia. Cancer Genet Cytogenet 1991;54:119–26.

[9] Sawyer JR, Roloson GJ, Head DR, Becton D. Karyotype evolution in a patient with Down syndrome and acute leukemia following a congenital leukemoid reaction. Med Pediatr Oncol 1994;22:404–9.

[10] Zipursky A, Wang H, Brown EJ, Squire J. Interphase cytogenetic analysis of in vivo differentiation in the myelodysplasia of Down syndrome. Blood 1994;84:2278–82.

[11] Yamaguchi Y, Fujii H, Kazama H, Iinuma K, Shinomiya N, Aoki T. Acute myeloblastic leukemia associated with trisomy 8 and translocation 8;21 in a child with Down syndrome. Cancer Genet Cytogenet 1997;97:32–4.

[12] Duflos-Delaplace D, Lai JL, Nelken B, Genevieve F, Defachelles AS, Zandecki M. Transient leukemoid disorder in a newborn with Down syndrome followed 19 months later by an acute myeloid leukemia: demonstration of the same structural change in both instances with clonal evolution. Cancer Genet Cytogenet 1999;113:166–71.

[13] Kojima S, Sako M, Kato K, Hosoi G, Sato T, Ohara A, Koike K, Okimoto Y, Nishimura S, Akiyama Y, Yoshikawa T, Ishii E, Okamura J, Yazaki M, Hayashi Y, Eguchi M, Tsukimoto I, Ueda K. An effective chemotherapeutic regimen for acute myeloid leukemia and myelodysplastic syndrome in children with Down's syndrome. Leukemia 2000;14:786–91.

[14] Creutzig U, Ritter J, Vormoor J, Ludwig WD, Niemeyer C, Reinisch I, Stollmann-Gibbels B, Zimmermann M, Harbott J. Myelodysplasia and acute myelogenous leukemia in Down's syndrome: a report of 40 children of the AML-BFM Study Group. Leukemia 1996;10:1677–86.

[15] Kaneko Y, Rowley JD, Variakojis D, Chilcote RR, Moohr JW, Patel D. Chromosome abnormalities in Down's syndrome patients with acute leukemia. Blood 1981;58:459–66.

[16] de Alarcon PA, Patil S, Golberg J, Allen JB, Shaw S. Infants with Down's syndrome: use of cytogenetic studies and in vitro colony assay for granulocyte progenitor to distinguish acute nonlymphocytic leukemia from a transient myeloproliferative disorder. Cancer 1987;60:987–93.

[17] Litz CE, Davies S, Brunning RD, Kueck B, Parkin JL, Gajl Peczalska K, Arthur DC. Acute leukemia and the transient myeloproliferative disorder associated with Down syndrome: morphologic, immunophenotypic and cytogenetic manifestations. Leukemia 1995;9: 1432–9.

[18] Blann MM, Morgan DL, Oblender M, Heinen B, Williams J, Tonk VS. Duplication of 1q in a child with Down syndrome and myelodysplastic syndrome. Cancer Genet Cytogenet 2000;119:74–6.

[19] Suarez CR, Le Beau MM, Silberman S, Fresco R, Rowley JD. Acute megakaryoblastic leukemia in Down's syndrome: report of a case and review of cytogenetic findings. Med Pediatr Oncol 1985;13: 225–31.

[20] Horsman DE, Massing BG, Chan KW, Kalousek DK. Unbalanced translocation (1;7) in childhood myelodysplasia. Am J Hematol 1988;27:174–8.

[21] Hoo JJ, Szego K, Jones B. Confirmation of centromeric fusion in 7p/1q translocation associated with myelodysplastic syndrome. Cancer Genet Cytogenet 1992;64:186–8.

[22] Zipursky A. Transient leukaemia: a benign form of leukaemia in newborn infants with trisomy 21. Br J Haematol 2003;120:930–8.

Cancer Science
The official journal of the Japanese Cancer Association JCA

# Dual antitumor mechanisms of Notch signaling inhibitor in a T-cell acute lymphoblastic leukemia xenograft model

Shigeo Masuda,[1,2,3] Keiki Kumano,[1,2] Takahiro Suzuki,[1,2] Taisuke Tomita,[4] Takeshi Iwatsubo,[4,5] Hideaki Natsugari,[6] Arinobu Tojo,[7] Makoto Shibutani,[8] Kunitoshi Mitsumori,[8] Yutaka Hanazono,[3] Seishi Ogawa,[1,9] Mineo Kurokawa[2] and Shigeru Chiba[1,10,11]

[1]Department of Cell Therapy and Transplantation Medicine, University of Tokyo Hospital, Tokyo; [2]Department of Hematology and Oncology, Graduate School of Medicine, University of Tokyo, Tokyo; [3]Division of Regenerative Medicine, Center for Molecular Medicine, Jichi Medical University, Tochigi; [4]Department of Neuropathology and Neuroscience, Graduate School of Pharmaceutical Sciences, University of Tokyo, Tokyo; [5]Department of Neuropathology, Graduate School of Medicine, University of Tokyo, Tokyo; [6]Department of Rational Medicinal Science, Graduate School of Pharmaceutical Sciences, University of Tokyo, Tokyo; [7]Department of Hematology and Oncology, Institute of Medical Sciences, University of Tokyo, Tokyo; [8]Laboratory of Veterinary Pathology, Tokyo University of Agriculture and Technology, Tokyo; [9]21th Century COE Program, Graduate School of Medicine, University of Tokyo, Tokyo; [10]Department of Clinical and Experimental Hematology, Graduate School of Comprehensive Human Sciences, University of Tsukuba, Tsukuba, Japan

(Received May 04, 2009/Revised August 19, 2009/Accepted August 21, 2009/Online publication September 23, 2009)

**Constitutive activation of Notch signaling is required for the proliferation of a subgroup of human T-cell acute lymphoblastic leukemias (T-ALL). Previous *in vitro* studies have demonstrated the therapeutic potential of Notch signaling inhibitors for treating T-ALL. To further examine this possibility, we applied a γ-secretase inhibitor (GSI) to T-ALL xenograft models. Treatment of established subcutaneous tumors with GSI resulted in partial or complete regression of tumors arising from four T-ALL cell lines that were also sensitive to GSI *in vitro*. To elucidate the mechanism of action, we transduced DND-41 cells with the active form of Notch1 (aN1), which conferred resistance to *in vitro* GSI treatment. Nevertheless, *in vivo* treatment with GSI induced a partial but significant regression of subcutaneous tumors that developed from aN1-transduced DND-41 cells, whereas it induced complete regression of tumors that developed from mock-transduced DND-41 cells. These findings indicate that the remarkable efficacy of GSI might be attributable to dual mechanisms, directly via apoptosis of DND-41 cells through the inhibition of cell-autonomous Notch signaling, and indirectly via disturbance of tumor angiogenesis through the inhibition of non-cell-autonomous Notch signaling. (*Cancer Sci* 2009; 100: 2444–2450)**

The Notch signaling pathway has a crucial role in a variety of cellular functions, including cell proliferation, differentiation, and apoptosis.[1,2] Notch proteins are heterodimeric transmembrane receptors composed of an extracellular subunit and a transmembrane subunit, and associate with each other via heterodimerization (HD) domains in the extracellular regions. Notch signaling, initiated by receptor-ligand interactions, requires subsequent proteolytic cleavage of the receptor by several proteases, resulting in liberation of the cleaved form of Notch1 that is functionally active (hereafter referred to as aN1) as it translocates into the nucleus and up-regulates the transcription of Notch-RBP-Jκ-regulated genes.[3]

Recent studies in tumorigenesis of hematologic malignancies and solid tumors have revealed several examples of aberrant Notch signaling.[2,4,5] Forced expression of aN1 in mouse bone marrow results in the development of T-cell leukemia,[6] and more importantly, amplified Notch signaling contributes to approximately 50% of human T-cell acute lymphoblastic leukemia (T-ALL).[7,8] The Notch signal amplification in T-ALL is due to gain-of-function mutations in the *NOTCH1* gene, which have also been detected in many different murine T-ALL models.[9–12] *NOTCH1* activating mutations cluster at the HD and intracellular domains, leading to ligand-independent cleavage and activation of Notch1, and increased stability of aN1, respectively. Notch1 signaling, whether initiated by receptor–ligand interactions or triggered by *NOTCH1*-activating mutations in the HD domains, eventually depends on the proteolytic activity of γ-secretase. γ-Secretase inhibitors (GSIs), available as small molecular compounds, suppress Notch signaling by blocking the activity of the γ-secretase complex.[13] Previous studies have demonstrated that blockade of Notch signaling with GSI induces cell cycle arrest and apoptosis in a subset of human T-ALL cell lines,[7,14,15] and an early phase clinical trial has already been conducted.[16] Despite that, precise mechanisms of action of GSI on T-ALL *in vivo* are yet to be elucidated.

Here, to examine the potential clinical applications for GSIs in T-ALL patients, and to evaluate the mechanisms of GSI action, we investigated the effects of the GSI compound YO01027[17] (referred to hereafter as YO) on human T-ALL growth in murine xenograft models, because YO administration to mice induced defective melanocyte stem cell maintenance but kept the mice otherwise healthy as shown in our previous paper.[18] The results here indicated that YO is highly effective against T-ALL growth *in vivo* and demonstrated that the efficacy of GSI might be due to the inhibition of Notch signaling via two mechanisms.

## Materials and Methods

**Cell cultures and reagents.** Human T-ALL cell lines (ALL-SIL, DND-41, HPB-ALL, KOPT-K1, TALL-1, MOLT-4, PF-382, and CEM) were obtained from the Fujisaki Cell Center, Hayashibara Biochemical Laboratories (Okayama, Japan), maintained in RPMI supplemented with 10% fetal bovine serum and penicillin/streptomycin, and incubated at 37°C with 5% $CO_2$. Human umbilical vein endothelial cells (HUVEC; Lonza Walkersville, Walkersville, MD, USA) were cultured in Endothelial Basal Medium-2 (Lonza Walkersville) and SingleQuots (Lonza Walkersville). The YO, which is an LY-411,575 analogue, was synthesized as described previously.[17] YO was dissolved in dimethyl sulfoxide (DMSO) to create 10 mM or 50 mM stock solutions.

**Animals.** SCID mice (C.B-17/Icr-*scid*/*scid*Jcl; 6 weeks old, female) were purchased from CLEA Japan (Tokyo, Japan) and

[11]To whom correspondence should be addressed. E-mail: schiba-tky@umin.net



doi: 10.1111/j.1349-7006.2009.01328.x

maintained under specific pathogen-free conditions. All experimental procedures were performed in accordance with the guidelines for animal experiments of the University of Tokyo and Jichi Medical University.

**Xenograft mouse model.** SCID mice at 6–8 weeks of age were inoculated subcutaneously in the right flank with $3 \times 10^7$ cells in 300 μL of phosphate buffered saline. In concurrent administration experiments, the mice were assigned to a control group and a YO-treated group the day after tumor inoculation. YO was orally administered daily for at least 30 days at a dose of 0.1 or 1 mg/kg/day. In challenge experiments for established tumors, mice were similarly assigned as described above at approximately 2.5–3 weeks (in HPB-ALL and TALL-1) or 8–12 weeks (in ALL-SIL and DND-41) after tumor cell inoculation, when tumor size had reached a certain volume. YO was orally administered daily at a dose of 0.1, 1, or 10 mg/kg/day. Tumor size was measured at the greatest length and width. The volume was calculated as $1/2 \times (\text{tumor length}) \times (\text{tumor width})^2$.

***In vivo* administration of YO.** *In vivo* administration of YO was performed as described previously.[19] Briefly, 0.1–10 mg/kg of YO or an equal volume of vehicle (DMSO) in 300 μL of 0.5% methylcellulose (Wako, Osaka, Japan) was administered orally to SCID mice using a disposable oral zonde (Fuchigami, Kyoto, Japan) once a day for the indicated periods.

**Plasmid construction and retroviral transduction.** The cDNA for myc-tagged murine aN1[20] was subcloned into the *Bam*HI restriction site of the retrovirus vector pMYs/internal ribosomal entry site-enhanced green fluorescent protein (IRES-EGFP; pMYs/IG).[21] Retroviral transduction of a human T-ALL cell line, DND-41, was performed using PLAT-F cells as described previously.[21] Following transduction, GFP-positive cells were sorted to 90% purity and used for further analysis. The proteins were detected by Western blotting using an anti-myc antibody (9E10).

**Proliferation assay.** Cell growth was quantified using a WST-1-based assay (Cell Counting Kit-8; Dojindo Medical Technologies, Kumamoto, Japan), which is a highly sensitive colorimetric assay. Briefly, human T-ALL cell lines ($3 \times 10^4$ cells/well) or HUVEC ($4 \times 10^3$ cells/well) were seeded into 96-well plates. Vascular endothelial growth factor (VEGF; 100 ng/mL) was supplemented in the medium for HUVEC. Various concentrations of YO were added, and proliferation was measured in duplicate at 7 days or 11 days using a WST-1-based assay according to the manufacturer's instructions. Proliferation was expressed as a percentage or fold change of vehicle-treated controls. Results are expressed as mean value ± SD.

**Detection of apoptosis.** Cells were incubated with various concentrations of YO for the indicated periods. Apoptosis was assessed using a fluorescein isothiocyanate-labeled Annexin V staining kit (Immunotech; Beckman-Coulter, Prague, Czech Republic) combined with 7-amino-actinomycin D (7-AAD), according to the manufacturer's instructions, with a FACS Calibur cytometer (BD Biosciences, San Jose, CA, USA).

**TUNEL staining.** To detect apoptotic cells, ALL-SIL-bearing SCID mice were sacrificed after the treatment with 1 mg/kg YO or vehicle for 5 days. Frozen blocks of tumors were cryosectioned and fixed with 1% paraformaldehyde, followed by analysis for apoptosis using the ApopTag Plus Peroxidase *In Situ* Apoptosis Detection Kit (Millipore, Billerica, MA, USA) according to the manufacturer's instructions.

**Western blotting.** Western blotting was performed as described previously.[22] The probes used were antibodies against cleaved Notch1 (Val1744; Cell Signaling Technology, Danvers, MA, USA) and GAPDH as a control. The Val1744 antibody was incubated at a dilution of 1:1000 overnight.

**Tube formation assay.** Upon the BD BioCoat Angiogenesis Plate (96 well), $2 \times 10^4$ HUVEC were seeded per well, with or without 100 nM YO. After 18 h, cells were stained with fluores-

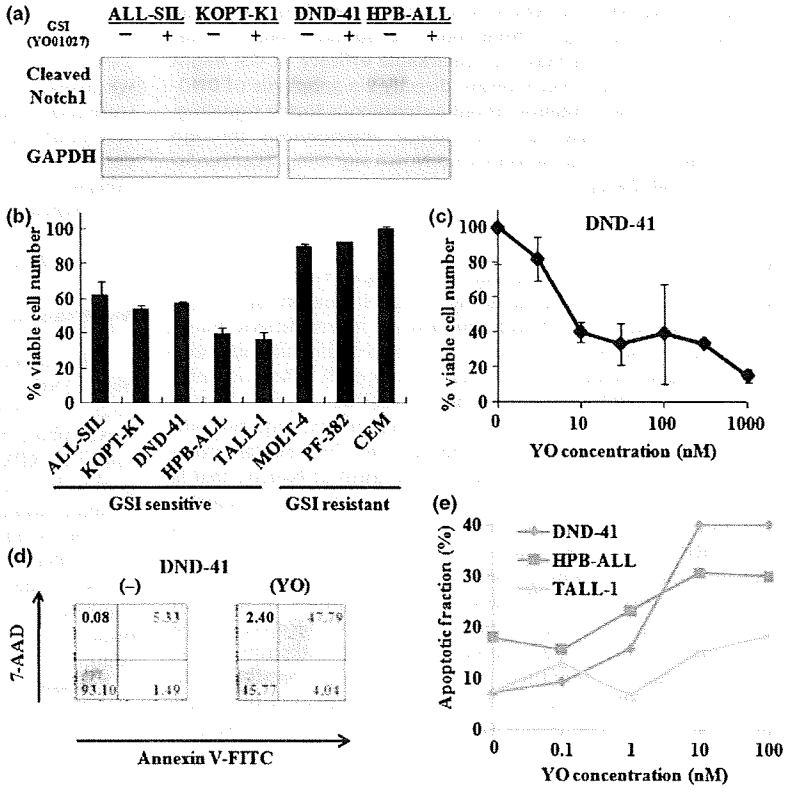


**Fig. 1.** Inhibition of Notch signaling impairs growth of human T-cell acute lymphoblastic leukemias (T-ALL) cell lines. (a) Western blot analysis for cleaved Notch1 in human T-ALL cell lines treated with 100 nM YO01027 for 48 h. GAPDH is shown as a loading control. (b) Proliferation assay of a panel of human T-ALL cell lines treated for 7 days with 100 nM YO01027 or vehicle control. The percent of viable cell number indicates the proportion of viable cells in the treated populations relative to untreated populations. (c) Dose dependent effects of YO01027 on the proliferation of DND-41 cell line treated for 7 days with 3, 10, 30, 100, 300, 1000 nM YO01027 or vehicle control. The percent of viable cell number indicates the proportion of viable cells in the treated populations relative to untreated populations. (d) Annexin V assay of DND-41 cell line treated for 7 days with 10 nM YO01027 or vehicle control. (e) Dose dependent effects of YO01027 on the apoptosis of human T-ALL cell lines treated for 7 days with 0.1, 1, 10, 100 nM YO01027 or vehicle control. The apoptotic fraction denotes the fraction of Annexin V (+)/7-AAD (+) cells, and the percent of apoptotic fraction indicates the proportion of apoptotic cells among the total cells within each treated well.

cent dye, Calcein AM (BD Biosciences), according to the manufacturer's instructions. Images were captured with the BIOREVO BZ-9000 microscope (Keyence, Osaka, Japan), and the tube length was measured using the BZ-H1C image analysis application (Keyence).

**Histological analysis.** Frozen blocks were cryosectioned at 5 μm and mounted on slides. Histological sections were air-dried and fixed in acetone for 15 min, followed by immunostaining with a 1:200 dilution of antimouse CD31 antibody (clone; MEC13.3) (BD-Pharmingen, San Diego, CA, USA) overnight at 4°C. Horseradish peroxide with the coloring agent diaminobenzidine was used as the substrate. Sections were then counterstained with hematoxylin. Vessel counting was performed at ×40 magnification in several randomly chosen areas.

**Statistics.** Statistical analyses were performed using the Student's *t*-test. A *P*-value of <0.05 was considered statistically significant.

## Results

**Human T-ALL lines are susceptible to Notch inhibition.** Some human T-ALL cell lines with *NOTCH1* activating mutations are sensitive to GSI *in vitro*.[7,13–15] We examined the ability of YO, a GSI compound that has not been tested in cell-based experiments, to inhibit Notch signaling. Various human T-ALL cell lines (ALL-SIL, KOPT-K1, DND-41, and HPB-ALL) were treated with YO for 48 h followed by immunoblotting with cleaved Notch1 (Val1744) antibody, which can specifically detect the aN1 proteins. Treatment of these cell lines with 100 nM YO resulted in an almost complete block of Notch1 activity (Fig. 1a).

To investigate the anti-proliferative effect of YO on T-ALL cells, we measured cellular viability using the WST-1-based assay in human T-ALL cell lines after YO treatment. As expected, YO exerted an anti-proliferative effect on some T-ALL cell lines (ALL-SIL, KOPT-K1, HPB-ALL, DND-41, and TALL-1), whereas other cell lines (MOLT-4, PF-382, and CEM) were not sensitive to this compound (Fig. 1b). To examine concentration dependency, DND-41 was treated with various concentrations of YO for 7 days and applied to the WST-1-based assay. A steep concentration dependency was observed between 1 nM and 10 nM. The effect was virtually saturated at >10 nM (Fig. 1c).

Next, we explored whether the decreased proliferation of T-ALL cell lines after treatment with YO was due to the induction of cell cycle arrest and/or apoptosis. We analyzed the cell cycle of the T-ALL cell lines after YO treatment using flow cytometry. As expected from previous reports,[7,13–15] YO induced G0-G1 arrest in all the T-ALL cell lines sensitive to YO (data not shown). Then, we treated five T-ALL cell lines with YO for 7 days followed by Annexin V/7-AAD staining, and found that YO induced significant apoptosis of DND-41 cells (Fig. 1d), as well as the other T-ALL cell lines tested (Fig. 1e). Similar results were observed using a pharmacologically distinct GSI, DAPT, known to block Notch activation (data not shown). Taken together, these results confirmed that some human T-ALL cell lines are susceptible to YO treatment *in vitro*.

**Concurrent administration of YO with tumor inoculation results in the inhibition of tumor growth in T-ALL xenograft models.** To examine *in vivo* antitumor effects of YO, we used murine xenograft models, in which SCID mice were inoculated subcutaneously with human cell lines. HPB-ALL and TALL-1 cell lines established subcutaneous tumors 2.5–3 weeks after inoculation. The subcutaneous tumors of the YO-treated groups were significantly smaller than those of control groups 2.5–4 weeks after the inoculation and the initiation of concurrent administration of YO or vehicle. Notably, in mice treated with 1 mg/kg of YO, there was no tumor formation observed in

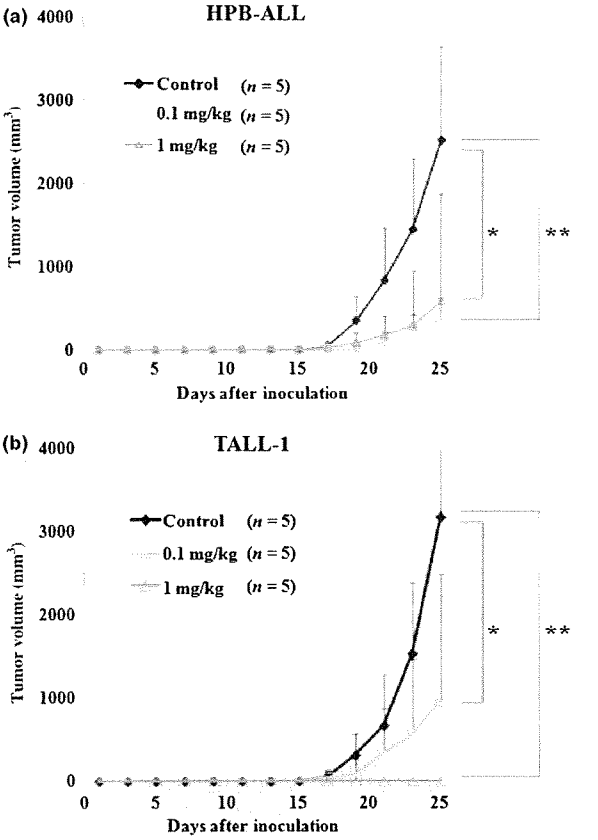


Fig. 2. Antitumor effects of YO01027 (YO) on xenograft models of human T-cell acute lymphoblastic leukemias (T-ALL), with concurrent administration of YO with tumor inoculation. Mice were inoculated subcutaneously with HPB-ALL (a) or TALL-1 cell lines (b). The next day, mice were randomly assigned to receive vehicle alone or varying doses of YO01027 daily, as described in "Materials and Methods". Data represent the mean tumor volume ($mm^3$) ±SD grown in vehicle-treated mice, YO (0.1 mg/kg)-treated mice, or YO (1 mg/kg)-treated mice. *$P < 0.05$; **$P < 0.01$, statistically significant differences (vehicle *vs* YO).

any of the TALL-1-inoculated mice or in approximately half the HPB-ALL-inoculated mice (Fig. 2a,b). This result indicates that YO exerts *in vivo* antitumor effects on T-ALL, at least during the period of tumor engraftment.

**YO treatment against established tumors in T-ALL xenograft models results in partial or complete regression.** Next, we evaluated the effects of YO treatment when the tumors grew to visible sizes. In this experimental design, YO treatment resulted in partial (HPB-ALL) or complete (ALL-SIL, DND-41, and TALL-1) regression of the established subcutaneous tumors. When treated with 10 mg/kg/day YO, the growth of tumors derived from HPB-ALL was suppressed to <50% compared with growth without treatment. Tumors derived from ALL-SIL, DND-41, and TALL-1 completely regressed within 2–3 weeks following treatment with YO at 1 mg/kg/day (Fig. 3a).

To confirm the *in vivo* pharmacologic inhibition of Notch signaling by YO, we excised tumors made of ALL-SIL from mice with or without 1 or 10 mg/kg/day YO treatment for 3 days, followed by immunoblotting of the tumor lysates with the Val1744 antibody. The level of cleaved Notch1 was reduced partially or almost completely after 1 or 10 mg/kg/day YO treatment, respectively. Thus, YO administered at both


doi: 10.1111/j.1349-7006.2009.01328.x

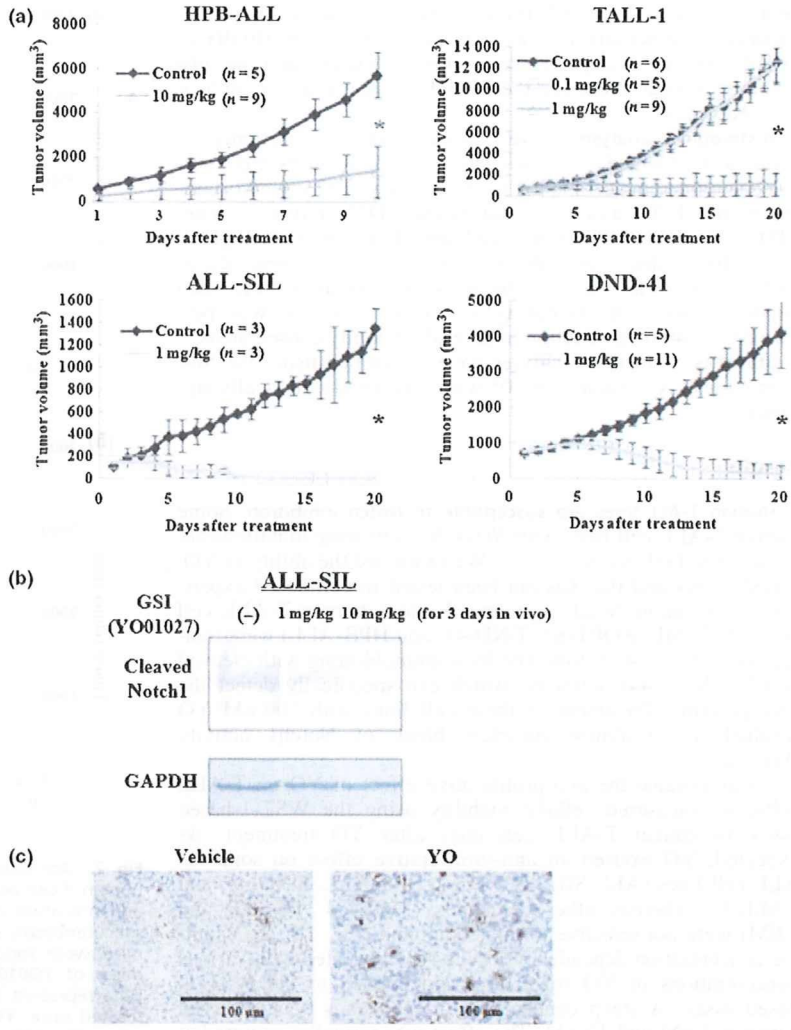


Fig. 3. Antitumor effects of YO01027 (YO) on xenograft models of human T-cell acute lymphoblastic leukemias (T-ALL), with YO treatment after tumor establishment. (a) Mice were inoculated subcutaneously with HPB-ALL, TALL-1, DND-41, or ALL-SIL cell lines. When the diameter of the tumor reached 12–13 mm, mice were randomly assigned to receive vehicle alone or varying doses of YO01027 daily, as described in the "Materials and Methods". Data represent the mean tumor volume ($mm^3$) ±SD grown in vehicle-treated mice or YO (0.1 or 1 or 10 mg/kg)-treated mice. *$P < 0.001$, statistically significant differences (vehicle *vs* YO). (b) Western blot analysis for cleaved Notch1 in engrafted tumors treated with YO. ALL-SIL-challenged mice were treated daily with vehicle alone or YO, and tumors were harvested 72 h after the initiation of treatment, followed by Western blotting of tumor lysates with cleaved Notch1 (Val1744) antibody. GAPDH is shown as a loading control. (c) YO treatment induces apoptosis of ALL-SIL cells *in vivo*. ALL-SIL-bearing mice were treated daily with vehicle alone or YO01027 at a dose of 1 mg/kg, and tumors were harvested 5 days after the initiation of treatment. Tumor sections were fixed with 1% paraformaldehyde and apoptotic cells were stained using TUNEL assay.

1 mg/kg/day and 10 mg/kg/day to SCID mice was pharmacologically active, and blocked Notch1 signaling partially or almost completely, at least in cells of subcutaneous tumors (Fig. 3b).

To determine whether YO treatment induces apoptosis *in vivo*, we performed TUNEL staining on tumors made of ALL-SIL, which was isolated from vehicle- or YO-treated mice. TUNEL-positive cells were reproducibly increased in number by the YO treatment (Fig. 3c), demonstrating increased apoptosis of T-ALL cells *in vivo*.

**Effect of aN1 expression in tumor growth during YO treatment.** We next expressed aN1 exogenously in DND-41 cell lines to examine whether aN1 rescues YO-induced cell growth arrest and tumor regression. aN1 represents a protein that is already cleaved, and is thus not a substrate for γ-secretase. Therefore, it was expected that DND-41 cells transduced with aN1 (hereafter referred to as DND-41/aN1) would become resistant to YO treatment.

We established DND-41/aN1 cells by infection of parental DNA-41 cells with aN1-expressing retrovirus, followed by bulk sorting of GFP-positive cells. Expression of aN1 proteins was confirmed by Western blotting with an anti-myc antibody (Fig. 4a). Parental DND-41 and mock-infected DND-41 (DND-41/mock) were sensitive to YO, but, as expected, DND-41/aN1 was substantially resistant to YO *in vitro* when assessed by a cell proliferation assay (Fig. 4b). The continuous presence of 100 nM YO allowed for selection of cells highly resistant to YO (DND-41/aN1/GSI; Fig. 4b). The *in vitro* growth curves of these cells under basal conditions (without YO) were very similar to each other (data not shown).

We implanted parental DND-41, DND-41/mock, DND-41/aN1, and DND-41/aN1/GSI cells subcutaneously into SCID mice. Subcutaneous tumors began to be palpable and the tumor volume reached 700 $mm^3$ in 8–12 weeks. Treatment with YO at 1 mg/kg/day or control vehicle was then initiated. In vehicle-treated mice, the tumors derived from parental DND-41, DND-41/mock, DND-41/aN1, and DND-41/aN1/GSI cells grew in a similar manner, whereas YO treatment resulted in a substantial regression of the tumors derived from parental DND-41 and DND-41/mock cells (Fig. 4c,d). Interestingly, *in vivo* YO treatment of tumors derived from DND-41/aN1 and DND-41/aN1/GSI cells, which were resistant to YO *in vitro*, induced significantly slower cell growth compared with the vehicle treatment, suggesting that these cells were sensitive to YO to some degree *in vivo* (Fig. 4c,d). In some mice, we observed a stabilization of the tumor volume. Nevertheless, YO treatment was not sufficiently effective on DND-41/aN1 and DND-41/aN1/GSI to regress the tumors to an impalpable level, unlike parental DND-41- and DND-41/mock-derived tumors.

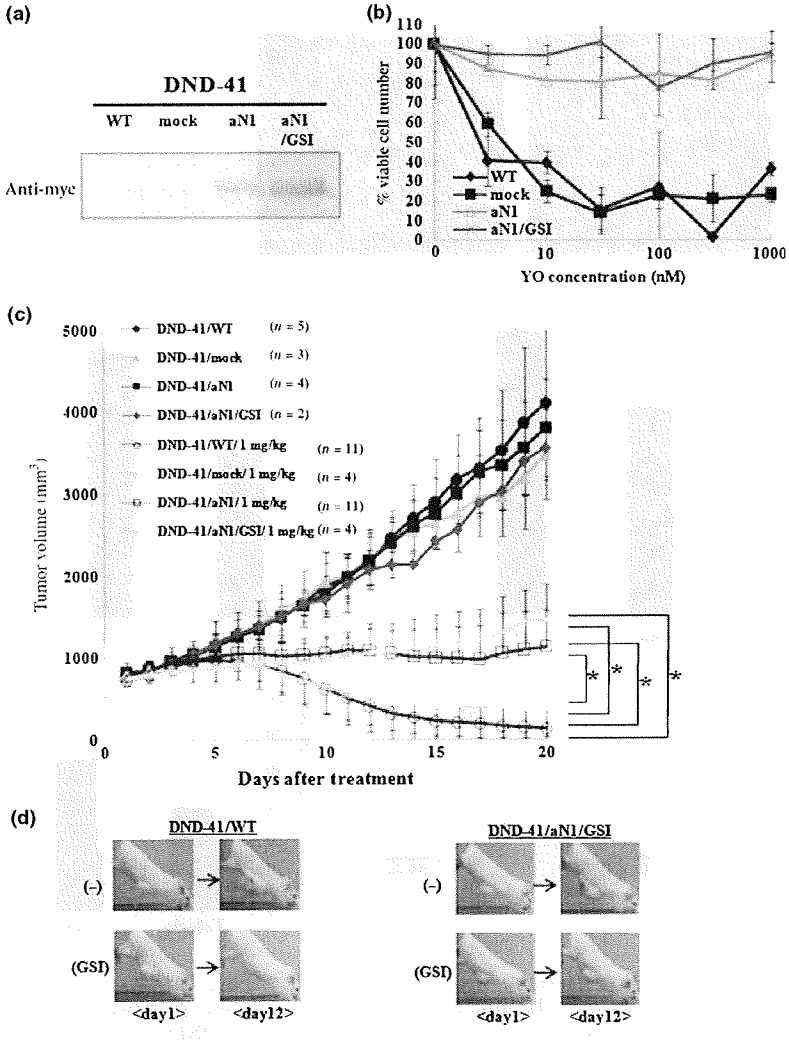


Fig. 4. Establishment of DND-41/aN1 and effects of aN1 rescue on tumor growth during YO01027 (YO) treatment. (a) Expression of aN1 proteins tagged with myc in DND-41/aN1 cells and DND-41/aN1/GSI cells was confirmed by Western blotting analysis. (b) Proliferation assay of established DND-41/aN1 and DND-41/aN1/GSI cell lines, compared with DND-41/WT and DND-41/mock cell lines, after treatment for 11 days with varying doses of YO. The percent of viable cell number indicates the proportion of viable cells in the treated populations relative to untreated populations. (c) Antitumor effects of YO on xenograft models of DND-41/WT, DND-41/mock, DND-41/aN1, and DND-41/aN1/GSI (pre-selected by γ-secretase inhibitor [GSI] *in vitro*). "1 mg/kg/day" denotes the group that received the YO treatment at a dose of 1 mg/kg/day. Data represent the mean tumor volume ($mm^3$) ±SD of vehicle-treated mice or YO (1 mg/kg)-treated mice. *$P < 0.01$, statistically significant differences. (d) Representative appearance of subcutaneous xenograft models during YO treatment. DND-41 cells stably expressing control vector or aN1 (pre-selected by GSI *in vitro*) were grown as xenografts in SCID mice. Representative mice from each group are shown.

**Effect of YO on *in vitro* tube formation and *in vivo* tumor vessels.** Recent studies have demonstrated that inhibition of Notch signaling in solid tumors resulted in tumor regression via increased tumor vessels with poor perfusion.[23–26] It has been shown that Notch inhibition leads to promotion of non-functioning angiogenesis.

Tube formation assay was performed to investigate the effect of YO on *in vitro* angiogenesis using HUVEC. We found that YO treatment significantly increased the tube length in the tube formation assay (Fig. 5a,b), suggesting that Notch inhibition promoted proliferation of endothelial cells, which is consistent with previous studies.[24,27] In addition, cell proliferation in the presence of VEGF was measured with WST-1-based assay. YO significantly promoted proliferation of HUVEC (Fig. 5c) as previously reported.[24,27]

To further clarify the mechanism of action with YO treatment, we analyzed the tumor vasculature during YO treatment. We implanted DND-41 cells into SCID mice and started YO or vehicle treatment after the tumor diameter reached approximately 1 cm. We sacrificed mice at treatment day 5, and analyzed tumor sections by immunostaining for anti-CD31, which is able to identify the vessels in tumors. In the average, approximately 30 and >40 vessels per $mm^2$ were observed in the vehicle-treated and YO-treated mice, respectively (Fig. 5d,e). These results are consistent with the previous reports described above, in which tumor regression would result from increased but poorly functional tumor vessels. Collectively, tumor regression in our models may depend partially on the disrupted tumor vasculature with paradoxically increased tumor vessels presumably through the inhibition of non-cell-autonomous Notch signaling by YO.

## Discussion

The findings of the present study confirmed that the YO compound that we synthesized is a GSI that efficiently blocks Notch signaling in T-ALL cell lines carrying activating *NOTCH1* mutations and induces apoptosis of these cell lines *in vitro*. The cell-autonomous effect against Notch signaling described here is postulated to be the mechanism of anti-T-ALL, creating the bases for clinical studies of a GSI targeting T-ALL.

We demonstrated a marked *in vivo* effect of YO in a xenograft model that was more dramatic than we had expected. Although the mechanisms of YO action on T-ALL have been virtually confined to the cell-autonomous Notch signal inhibition, including a recent report describing the combinatorial effect of steroid with GSI,[28] the strong effect of GSI *in vivo* could also be attributed to non-cell-autonomous inhibition of Notch signaling.

Our findings were consistent with the recent reports on the role of Notch signaling in tumor angiogenesis.[23–26] Delta-4, one of the Notch ligands, is expressed on tip cells in the endothe-


doi: 10.1111/j.1349-7006.2009.01328.x

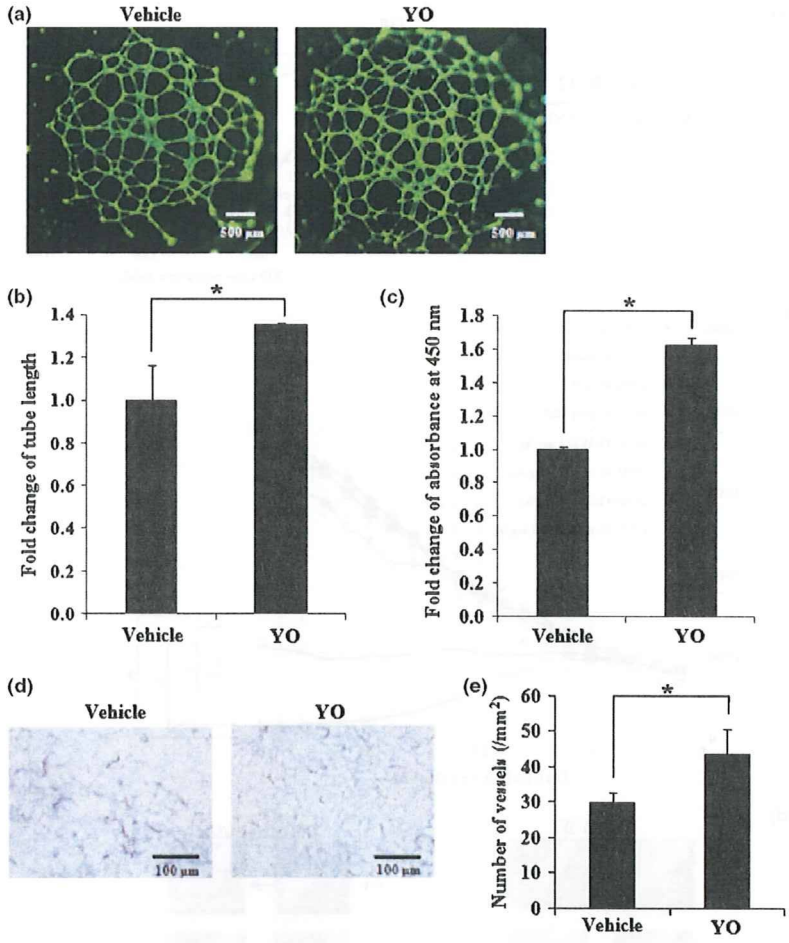


Fig. 5. *In vitro* and *in vivo* analysis of vascular cells after YO01027 (YO) treatment. (a) The *in vitro* tube formation analysis of HUVEC, either with or without 100 nM YO treatment. The cells were stained with fluorescent dye, Calcein AM, and the representative images are shown. Original magnification, ×20. (b) Quantitative analysis of tube length after tube formation of HUVEC with or without 100 nM YO. Fold change of tube length is shown, compared with that of vehicle control. $*P < 0.05$, statistically significant differences. (c) The cell proliferation assay of HUVEC in the presence of vascular endothelial growth factor (VEGF), either with or without 100 nM YO for 7 days. Fold change of absorbance at 450 nm is shown, compared with that of the vehicle control. $*P < 0.05$, statistically significant differences. (d) Anti-CD31 immunostainings of tumor sections in DND-41-bearing SCID mice, either after YO treatment at a dose of 1 mg/kg/day or after vehicle treatment. Original magnification, ×40. (e) Quantitative analysis of vessels in tumors after YO treatment. The cells stained with anti-CD31 were counted, and data represent the mean vessel density (per $mm^2$) ±SD in tumors derived from DND-41. $*P < 0.05$, statistically significant differences.

lium of newly elongating tumor vessels by stimulation with VEGF. Engagement of Notch1 expressed on the stalk cells in the endothelium by neighboring tip cell-expressing Delta-4 blocks differentiation of the stalk cells into tip cells, which represents the process required for the normally functioning tumor vessel formation. Blockade of this signaling pathway impairs normal tumor angiogenesis and creates hyper-blanched, non-functioning vasculature, which results in regression of the solid tumor. Whereas we used T-ALL cell lines in our experiments, we chose the subcutaneous tumor injection model because it is more convenient for observing and measuring the tumors. In this subcutaneous tumor model, we observed a similar tendency regarding tumor vessel density, from which we could easily speculate that the same mechanism was underlying this phenomenon.

The introduction of the GSI-insensitive cleaved form of Notch1 into DND-41 cells transformed these cells to be completely resistant to YO *in vitro*, exactly as expected, but failed to confer complete resistance to YO in the subcutaneous xenograft model. Whereas the subcutaneous tumors derived from DND-41/aN1 were significantly more resistant to YO than tumors derived from parental DND-41 and DND-41/mock cells, they still significantly responded to YO. These observations fit the idea that the marked *in vivo* antitumor effect of YO against subcutaneous tumors derived from parental DND-41 as well as DND-41/mock cells was mediated through, in addition to the cell-autonomous effect, a blockade of tumor vasculature that supplies blood to the tumor cells in a non-cell-autonomous fashion.

We confirmed that subcutaneous tumors made of a colon cancer cell line, LoVo, which was non-sensitive to YO *in vitro*, were partially regressed by YO at 10 mg/kg/day (data not shown). The effect of YO on the LoVo tumors, however, was not as strong as on tumors made of parental DND-41 and several other T-ALL cell lines, again supporting the idea that the exceptionally strong effect of YO on T-ALL xenografts is due to the inhibiting effect of YO on Notch signaling at two independent targets *in vivo*.

As shown in Figure 3(b), inhibition of Notch1 activation *in vivo* was almost complete with YO at 10 mg/kg but incomplete with YO at 1 mg/kg. On the other hand, the effect of YO *in vitro* was saturated by YO >10 nM, as shown in Figure 1(c). These findings might indicate that >10 nM serum/tissue concentration is achieved with 10 mg/kg and 1–10 nM with 1 mg/kg administration, if both *in vitro* and *in vivo* results are considered together. Whereas administration of YO at 1–3 mg/kg/day for up to 4 weeks did not cause weight loss, diarrhea, or hair coat abnormalities in mice, treatment at 10 mg/kg/day for more than 2 weeks resulted in obvious weight loss, diarrhea, and hair coat roughness. This implies a narrow window of YO for the treatment purpose. Nevertheless, it also indicates that the sensitivity to YO is variable among tissues and cells, and this difference might be important for YO to be considered as a drug. Together with the results described in previous papers,[18,29,30] a subset of T-ALL cells may be the most sensitive among others and possibly similar to melenocyte stem cells and splenic marginal zone B cells. In contrast, thymocyte progenitors and intestinal goblet cells appear to be less sensitive to YO.

Based on the facts that subcutaneous tumors from T-ALL cell lines do not represent common clinical presentations and that

our finding might depend on the experimental model that we chose in this study, the question arises as to how the current findings can be translated to clinical application. The vasculature component might be negligible in the leukemia model, but the effect of the combination of cell-autonomous apoptosis induction in leukemia cells with the inhibition of angiogenesis in leukemic cell-infiltrating bone marrow is not known. The effectiveness of YO in a leukemia model must be examined using the same T-ALL cell lines.

The discovery of *NOTCH1* activating mutations in T-ALL has made the Notch pathway an attractive target for therapy.[31] The results described here indicate the rationale for the use of GSI in the treatment of T-ALL, as well as for solid tumors whose tumor vasculature formation is dependent on Notch signaling.

Nevertheless, resistance of T-ALL against GSI might limit the clinical use of GSI. Recently, mutational loss of the phosphatase and tensin homolog (PTEN) gene, which encodes a key tumor suppressor that inhibits the phosphatidylinositol-3 kinase (PI3K)–Akt signaling pathway, was discovered in T-ALL cells that are resistant to GSI.[32] This could explain the variation of GSI sensitivity among T-ALL cells. Our results with HPB-ALL raise a different issue. This cell line was very sensitive to YO *in vitro*, but subcutaneous tumors derived from HPB-ALL appeared to be less sensitive to YO compared to other cells such as DND-41. This result indicates that YO concentrations sufficient to inhibit Notch1 activation may not be achieved in the subcutaneous tumor made from HPB-ALL. In addition, it is likely that inhibition of tumor vessel formation is less efficient for the reduction of subcutaneous HPB-ALL tumors for some reasons, such that this particular tumor is less dependent on tumor vessels.

Expectations and questions are intermingled with regard to the development of GSI and other Notch signal inhibitors for the treatment of T-ALL as well as other tumors. Nevertheless, various Notch signal inhibitors are being developed aiming at clinical use.

## Acknowledgments

We thank Toshio Kitamura (Institute of Medical Science, University of Tokyo) for the pMYs/IRES-EGFP retrovirus vector and Akira Harashima (Hayashibara Biomedical Laboratories) for the T-ALL cell lines (ALL-SIL, DND-41, HPB-ALL, KOPT-K1, TALL-1, MOLT-4, PF-382, and CEM). This work was supported in part by Grants-in-Aid for Scientific Research (KAKENHI nos. 17014023, 18013012, and 19390258) from the Ministry of Education, Culture, Sports, Science and Technology (MEXT) of Japan, and a Research Grant from the Sagawa Foundation of Promotion of Cancer Sciences to S.C.; Grants-in-Aid for Young Scientists (KAKENHI nos. 17790637 and 19790660) from MEXT; research funding for young scientists from the Science and Technology Foundation of Japan; research funding from the Japan Leukemia Research Fund; and research funding from Aichi Cancer Research Foundation to S.M.

## References

1 Grabher C, von Boehmer H, Look AT. Notch 1 activation in the molecular pathogenesis of T-cell acute lymphoblastic leukaemia. *Nat Rev Cancer* 2006; **6**: 347–59.
2 Leong KG, Karsan A. Recent insights into the role of Notch signaling in tumorigenesis. *Blood* 2006; **107**: 2223–33.
3 Mumm JS, Kopan R. Notch signaling: from the outside in. *Dev Biol* 2000; **228**: 151–65.
4 Pear WS, Aster JC. T cell acute lymphoblastic leukemia/lymphoma: a human cancer commonly associated with aberrant NOTCH1 signaling. *Curr Opin Hematol* 2004; **11**: 426–33.
5 Lee SY, Kumano K, Nakazaki K *et al.* Gain-of-function mutations and copy number increases of Notch2 in diffuse large B-cell lymphoma. *Cancer Sci* 2009; **100**: 920–6.
6 Pear WS, Aster JC, Scott ML *et al.* Exclusive development of T cell neoplasms in mice transplanted with bone marrow expressing activated Notch alleles. *J Exp Med* 1996; **183**: 2283–91.
7 Weng AP, Ferrando AA, Lee W *et al.* Activating mutations of NOTCH1 in human T cell acute lymphoblastic leukemia. *Science* 2004; **306**: 269–71.
8 Lee SY, Kumano K, Masuda S *et al.* Mutations of the Notch1 gene in T-cell acute lymphoblastic leukemia: analysis in adults and children. *Leukemia* 2005; **19**: 1841–3.
9 Dumortier A, Jeannet R, Kirstetter P *et al.* Notch activation is an early and critical event during T-Cell leukemogenesis in Ikaros-deficient mice. *Mol Cell Biol* 2006; **26**: 209–20.
10 Lin YW, Nichols RA, Letterio JJ, Aplan PD. Notch1 mutations are important for leukemic transformation in murine models of precursor-T leukemia/lymphoma. *Blood* 2006; **107**: 2540–3.
11 O'Neil J, Calvo J, McKenna K *et al.* Activating Notch1 mutations in mouse models of T-ALL. *Blood* 2006; **107**: 781–5.
12 Reschly EJ, Spaulding C, Vilimas T *et al.* Notch1 promotes survival of E2A-deficient T cell lymphomas through pre-T cell receptor-dependent and -independent mechanisms. *Blood* 2006; **107**: 4115–21.
13 Weng AP, Nam Y, Wolfe MS *et al.* Growth suppression of pre-T acute lymphoblastic leukemia cells by inhibition of notch signaling. *Mol Cell Biol* 2003; **23**: 655–64.
14 Lewis HD, Leveridge M, Strack PR *et al.* Apoptosis in T cell acute lymphoblastic leukemia cells after cell cycle arrest induced by pharmacological inhibition of Notch signaling. *Chem Biol* 2007; **14**: 209–19.
15 O'Neil J, Grim J, Strack P *et al.* FBW7 mutations in leukemic cells mediate NOTCH pathway activation and resistance to γ-secretase inhibitors. *J Exp Med* 2007; **204**: 1813–24.
16 Shih IeM, Wang TL. Notch signaling, γ-secretase inhibitors, and cancer therapy. *Cancer Res* 2007; **67**: 1879–82.
17 Fuwa H, Okamura Y, Morohashi Y *et al.* Highly efficient synthesis of medium-sized lactams via intramolecular Staudingeraza-Wittig reaction of w-azido pentafluorophenyl ester: synthesis and biological evaluation of Ly411575 analogues. *Tetrahedron Lett* 2004; **45**: 2323–6.
18 Kumano K, Masuda S, Sata M *et al.* Both Notch1 and Notch2 contribute to the regulation of melanocyte homeostasis. *Pigment Cell Melanoma Res* 2008; **21**: 70–8.
19 Wong GT, Manfra D, Poulet FM *et al.* Chronic treatment with the gamma-secretase inhibitor LY-411,575 inhibits beta-amyloid peptide production and alters lymphopoiesis and intestinal cell differentiation. *J Biol Chem* 2004; **279**: 12876–82.
20 Kumano K, Chiba S, Kunisato A *et al.* Notch1 but not Notch2 is essential for generating hematopoietic stem cells from endothelial cells. *Immunity* 2003; **18**: 699–711.
21 Kitamura T, Koshino Y, Shibata F *et al.* Retrovirus-mediated gene transfer and expression cloning: powerful tools in functional genomics. *Exp Hematol* 2003; **31**: 1007–14.
22 Masuda S, Kumano K, Shimizu K *et al.* Notch1 oncoprotein antagonizes TGF-beta/Smad-mediated cell growth suppression via sequestration of coactivator p300. *Cancer Sci* 2005; **96**: 274–82.
23 Noguera-Troise I, Daly C, Papadopoulos NJ *et al.* Blockade of Dll4 inhibits tumour growth by promoting non-productive angiogenesis. *Nature* 2006; **444**: 1032–7.
24 Ridgway J, Zhang G, Wu Y *et al.* Inhibition of Dll4 signalling inhibits tumour growth by deregulating angiogenesis. *Nature* 2006; **444**: 1083–7.
25 Hellstrom M, Phng LK, Hofmann JJ *et al.* Dll4 signalling through Notch1 regulates formation of tip cells during angiogenesis. *Nature* 2007; **445**: 776–80.
26 Siekmann AF, Lawson ND. Notch signalling limits angiogenic cell behaviour in developing zebrafish arteries. *Nature* 2007; **445**: 781–4.
27 Yamanda S, Ebihara S, Asada M *et al.* Role of ephrinB2 in nonproductive angiogenesis induced by Delta-like 4 blockade. *Blood* 2009; **113**: 3631–9.
28 Real PJ, Tosello V, Palomero T *et al.* Gamma-secretase inhibitors reverse glucocorticoid resistance in T cell acute lymphoblastic leukemia. *Nat Med* 2009; **15**: 50–8.
29 Radtke F, Wilson A, Stark G *et al.* Deficient T cell fate specification in mice with an induced inactivation of Notch1. *Immunity* 1999; **10**: 547–58.
30 Saito T, Chiba S, Ichikawa M *et al.* Notch2 is preferentially expressed in mature B cells and indispensable for marginal zone B lineage development. *Immunity* 2003; **18**: 675–85.
31 Aster JC. Deregulated NOTCH signaling in acute T-cell lymphoblastic leukemia/lymphoma: new insights, questions, and opportunities. *Int J Hematol* 2005; **82**: 295–301.
32 Palomero T, Sulis ML, Cortina M *et al.* Mutational loss of PTEN induces resistance to NOTCH1 inhibition in T-cell leukemia. *Nat Med* 2007; **13**: 1203–10.



doi: 10.1111/j.1349-7006.2009.01328.x

# Single nucleotide polymorphism genomic arrays analysis of t(8;21) acute myeloid leukemia cells

Tadayuki Akagi,[1] Lee-Yung Shih,[2,3] Seishi Ogawa,[4,5] Joachim Gerss,[6] Stephen R. Moore,[7] Rhona Schreck,[7] Norihiko Kawamata,[1] Der-Cherng Liang,[8] Masashi Sanada,[4,5] Yasuhito Nannya,[4] Stefan Deneberg,[1] Vasilios Zachariadis,[10] Ann Nordgren,[10] Jee Hoon Song,[1] Martin Dugas,[6] Sören Lehmann,[1,9] and H. Phillip Koeffler[1]

[1]Division of Hematology and Oncology, Cedars-Sinai Medical Center, UCLA School of Medicine, Los Angeles, CA, USA; [2]Division of Hematology-Oncology, Chang Gung Memorial Hospital, Taipei, Taiwan; [3]School of Medicine, Chang Gung University, Taoyuan, Taiwan; [4]Department of Hematology and Oncology and [5]the 21st century COE program, Graduate School of Medicine, University of Tokyo, Tokyo, Japan; [6]Department of Medical Informatics and Biomathematics, University of Munster, Munster, Germany; [7]Pathology/Laboratory Medicine and Medical Genetics Institute, Cedars-Sinai Medical Center, Los Angeles, CA, USA; [8]Department of Pediatrics, Mackay Memorial Hospital, Taipei, Taiwan; [9]Department of Hematology, and [10]Department of Clinical Genetics, Karolinska University Hospital, Stockholm, Sweden

## ABSTRACT

Translocation of chromosomes 8 and 21, t(8;21), resulting in the *AML1-ETO* fusion gene, is associated with acute myeloid leukemia. We searched for additional genomic abnormalities in this acute myeloid leukemia subtype by performing single nucleotide polymorphism genomic arrays (SNP-chip) analysis on 48 newly diagnosed cases. Thirty-two patients (67%) had a normal genome by SNP-chip analysis (Group A), and 16 patients (33%) had one or more genomic abnormalities including copy number changes or copy number neutral loss of heterozygosity (Group B). Two samples had copy number neutral loss of heterozygosity on chromosome 6p including the *PIM1* gene; and one of these cases had E135K mutation of Pim1. Interestingly, 38% of Group B and only 13% of Group A samples had a *KIT*-D816 mutation, suggesting that genomic alterations are often associated with a *KIT*-D816 mutation. Importantly, prognostic analysis revealed that overall survival and event-free survival of individuals in Group B were significantly worse than those in Group A.

Key words: t(8;21), *AML1-ETO*, CNN-LOH, SNP-chip, *KIT*, *PIM1*.

*Citation: Akagi T, Shih L-Y, Ogawa S, Gerss J, Moore SR, Schreck R, Kawamata N, Liang D-C, Sanada M, Nannya Y, Deneberg S, Zachariadis V, Nordgren A, Song JH, Dugas M, Lehmann S, and Koeffler HP. Single nucleotide polymorphism genomic arrays analysis of t(8;21) acute myeloid leukemia cells. Haematologica 2009;94:1301-1306. doi:10.3324/haematol.2009.005744*



## Introduction

The t(8;21)(q22;q22) translocation occurs in 40% of patients with acute myeloid leukemia (AML) of the FAB-M2 subtype, and constitutes 12% of all newly diagnosed cases of AML. This translocation leads to a fusion product of AML1 (also called RUNX1 or CBFβ) and ETO (also called MTG8). Data have suggested that the translocation is an early event in leukemogenesis.[1] Furthermore, the t(8;21) translocation can be found in neonatal Guthrie blood spots of infants that later developed *AML1-ETO* leukemia, suggesting that the translocation can precede development of AML by up to ten years.[2,3]

Several murine models have demonstrated that *AML1-ETO* alone is not sufficient to induce leukemia. Murine bone marrow cells expressing tetracycline-inducible *AML1-ETO* transgene did not develop leukemia:[4] but developed myeloproliferative disorders.[5] In contrast, 30-55% of *AML1-ETO*-expressing mice treated with the DNA-alkylating mutagen N-ethyl-N-nitrosourea (ENU) developed AML.[6,7] These findings strongly suggest that a secondary hit is necessary for the development of t(8;21) AML.

The protooncogene *KIT* is a receptor tyrosine kinase. Activating mutations of *KIT* including those in either the extracellular (exon 8) region or the protein kinase domains

*Acknowledgments: we thank members of our laboratories for helpful discussions. Funding: this work was supported by NIH grants, Parker Hughes Fund (HPK); and the grant support of NHRI-EX96-9434SI (LS) and MMH-E-96009 (DL). HPK is the holder of the Mark Goodson endowed Chair in Oncology Research and is a member of the Jonsson Cancer Center and the Molecular Biology Institute, UCLA. MD is supported by the European Leukemia Network (funded by the 6th Framework Program of the European Community). This article is dedicated to the memory of David Golde, a mentor and friend. Manuscript received on January 7, 2009. Revised version on arrived March 11, 2009. Manuscript accepted on March 25, 2009.*
*Correspondence: Tadayuki Akagi, Department of Stem Cell Biology, Graduate School of Medical Science, Kanazawa University, 13-1 Takara-machi, Kanazawa, Ishikawa 920-8640, Japan. E-mail: tadayuki@staff.kanazawa-u.ac.jp. Sören Lehmann, Department of Hematology M54, Karolinska University Hospital, Huddinge, Stockholm 141 86, Sweden. E-mail: soren.lehmann@ki.se.*
*The online version of this article contains a supplementary appendix.*

(D816 mutation) are found in 2% and 11% of t(8;21) AML samples, respectively.[8,9] FLT3 is also a receptor tyrosine kinase. Two frequent activating mutations of *FLT3*, FLT3-internal tandem duplication (ITD) and FLT3-tyrosine kinase domain (TKD) mutation, are detected in a range of 2-8% and 2-4% of samples of t(8;21) AML, respectively.[10,11] Mutation of *NRAS* at either codon 12, 13 or 61 is found in 9% of t(8;21) AML samples.[10,11]

High-density single nucleotide polymorphism genomic arrays (SNP-chip) allow the detection of copy number changes, as well as copy number neutral loss of heterozygosity (CNN-LOH) in leukemia samples.[12-18] In order to screen for secondary alteration(s) that potentially could cause *AML1-ETO* transformed cells to develop acute myeloid leukemia, we performed SNP-chip analysis of 48 t(8;21) AML samples. The use of CNAG (copy number analysis for Affymetrix GeneChips) program[12] and an algorithm AsCNAR (allele-specific copy number analysis using anonymous references)[18] allows identification of hidden abnormalities and novel disease-related genomic regions in the leukemia samples. Here, we found that genomic changes detected by SNP-chip analysis are associated with a poor overall and event-free survival in t(8;21) AML.

## Design and Methods

### Patient samples, determination of mutant genes and statistical analysis

Genomic DNA of 48 anonymized samples of t(8;21) AML cells were obtained from Chang-Gung Memorial Hospital, Chang-Gung University in Taiwan after obtaining informed consent. These samples had been frozen over a span of 14 years (July 1990 to July 2004). Sample information is shown in the *Online Supplementary Table S1*. The study has been approved by Cedars-Sinai Medical Center (IRB number 4485).

To detect an AML1-ETO fusion transcript, RT-PCR was performed using specific primers as described previously.[19] Mutation analysis of the *KIT* gene for the t(8;21) AML samples was reported previously.[20] Statistical analysis is described in the *Online Supplementary Design and Methods section.*

### SNP-chip analysis

Genomic DNA isolated from t(8;21) AML cells was subjected to GeneChip Human mapping microarray (SNP-chip, Affymetrix, Santa Clara, CA, USA) as described previously;[12,13] ten samples (cases #47, #51, #52, #54, #56, #57, #59, #60, #61 and #62) were examined with the 250 K array, and the other 38 samples were analyzed with the 50 K array. The allele-specific copy numbers (AsCNs) were estimated using normal genomic DNA from peripheral blood of normal volunteers as controls.[13] The array does not contain Y-chromosome probes; therefore, we summarize the SNP-chip data without sex chromosomes. Size, position and location of genes were identified with UCSC Genome Browser (*http://genome.ucsc.edu/*). Copy number changes previously described as copy number variants (*http://projects.tcag.ca/variation/*) were excluded.

### Fluorescence in situ hybridization (FISH) analysis

Interphase hybridizations were performed following the manufacturer's instructions and standard protocols. Probes for the *SNRPN* gene, 15q telomere, 7p telomere and 7q telomere were obtained from Cytocell (Cambridge, United Kingdom); and probes for the *MYC* gene as well as the centromere of chromosome 8 were purchased from Abbott Molecular (Abbott Park, IL, USA). Fifty interphase cells were scored for each sample, with 20 cells scored in controls (bone marrow controls with normal karyotypes). Signal patterns were normal for all controls with all probe sets.

### Analysis of the PIM1 gene

Six coding exons of the *PIM1* gene were amplified using specific primers from genomic DNA of cases #39 and #41. After purification of the PCR products from agarose gel, nucleotide sequences were determined. Primer sequences will be provided upon request. These 6 exons of other t(8;21) AML samples were examined by single strand conformation polymorphism (SSCP) as described in the *Online Supplementary Design and Methods* section.

To determine the frequency of missense mutations of the *PIM1* gene within exon 4, this region of 34 t(8;21) AML samples and 40 normal blood DNA samples were amplified by PCR using specific primer (5'-TCC TGG AGA GGC CCG AGC-3' and 5'-TTG AGG TCG ATA AGG ATG-3'). The PCR product (178 bp) was treated with a restriction enzyme Hpy188III for 1h. PCR products from wild-type allele are not digested but mutated allele are digested by the restriction enzyme.

## Results and Discussion

### SNP-chip analysis of 48 t(8;21) acute myeloid leukemia samples

SNP-chip analysis of 48 t(8;21) acute myeloid leukemia (AML) samples revealed several genomic copy number changes, as well as copy number neutral loss of heterozygosity (CNN-LOH). As shown in Table 1 and *Online Supplementary Figure S1*, 32 patients (67%) had a normal genome by SNP-chip analysis (Group A, mean age is 23, range 2-74). In contrast, 16 patients (33%) had one or more genomic abnormalities (Group B, mean age is 31, range 4-61). Thus, these copy number changes probably harbor dysregulated leukemia-associated genes in t(8;21) AML. Cytogenetics showed that case #33 had trisomy 4 in 2 out of 15 cells (13%), and case #34 had monosomy 18 in 6 out of 24 cells (25%) (*Online Supplementary Table S1*). These minor clones were not detected by SNP-chip analysis. Case #40 had tetraploidy in 23 out of 25 cells; 2-fold gene-dosage in all chromosomes was masked and detected as normal gene-dosage.

Next, we compared SNP-chip results and gene mutations. Ten out of 48 samples (18%) had a *KIT*-D816 mutation. Interestingly, 6 (case #7, #14, #26, #37, #40, and #52) of the 10 samples were found in Group B,

**Table 1.** Chromosomal regions with copy number changes and copy number neutral loss of heterozygosity in t(8; 21) acute myeloid leukemia samples.

| Case # | Status | Location | Physical localization | | Size (Mb) | Genes |
|---|---|---|---|---|---|---|
| | | | Proximal | Distal | | |
| 6 | Dup | 8q24.23 | 137,858,383 | 137,892,295 | 0.03 | No known genes |
| 7 | Dup | 18q21.32 | 56,209,691 | 56,315,439 | 0.1 | No known genes |
| | CNN-LOH | 11pter-p12 | 1,938,894 | 42,449,197 | 40.5 | >10 genes including *CDKN1C, HRAS,* and *WT1* |
| 13 | Tri | Trisomy 15 | – | – | – | >10 genes |
| 14 | Del | 7q35-q36.1 | 146,128,574 | 148,288,861 | 2.1 | *CNTNAP2, CUL1, EZH2, PDIA4, ZNF425, ZNF298* |
| 17 | Del | 9q13-q36.1 | 68,275,512 | 84,477,002 | 16.2 | >10 genes |
| 26 | Tri | Trisomy 4 | – | – | – | >10 genes including *KIT* |
| | Del | 13q21.1 | 54,339,313 | 54,457,753 | 0.1 | no known genes |
| 28 | Dup | 15q21.1-qter. | 46,526,374 | 100,182,183 | 53.7 | >10 genes |
| | Del | 16pter -p13.2 | 1,543,577 | 7,010,644 | 5.5 | >10 genes |
| 34 | Del | 7q31.2-qter. | 116,548,736 | 158,554,645 | 42 | >10 genes |
| | Dup | 8q22.1-qter. | 97,255,867 | 143,902,698 | 46.6 | >10 genes including *MYC* |
| | Del | 9q33.1 | 116,515,445 | 117,926,188 | 1.4 | *TNFSF15, TNFSF8, TNC, DEC1, CTS9, EST-YD1* |
| | Del | 9q13-q31.3 | 68,275,512 | 109,232,711 | 41 | > 10 genes |
| 37 | Dup | 4p16.1-q28.3 | 7,902,265 | 139,029,890 | 131.1 | >10 genes including *KIT* |
| | Dup | 8q22.1-qter. | 96,550,847 | 143,902,698 | 47.4 | >10 genes including *MYC* |
| 39 | Tri | Trisomy 4 | – | – | – | >10 genes including *KIT* |
| | Dup | 14q11.2-q13.1 | 19,285,288 | 33,978,199 | 14.7 | >10 genes |
| | CNN-LOH | 6pter-p12.3 | 150,610 | 46,902,007 | 46.8 | >10 genes including *PIM1* and *CDKN1A* |
| 40 | Mono | Monosomy 11 | – | – | – | >10 genes |
| 41 | CNN-LOH | 6p-ter. - 6p21.1 | 150,610 | 44,873,513 | 44.7 | >10 genes including *PIM1* and *CDKN1A* |
| 43 | Mono | Monosomy 7 | – | – | – | >10 genes |
| 52 | Dup | 5q14.1 | 77034347 | 77551493 | 0.5 | *TBCA, AP3B1* |
| 59 | CNN-LOH | 11q13.2 - q-ter. | 67259252 | 134439182 | 67.2 | >10 genes |
| | Del | 16q21 | 57560512 | 58960978 | 1.4 | no known genes |
| 60 | Dup | 1q41 - q-ter. | 211518337 | 245353397 | 33.8 | >10 genes |
| | Del | 7q31.32 | 121860398 | 122756128 | 0.9 | *CADPS2, RNF133, RNF148, AK058116, TAS2R16, SLC13A1* |
| | Del | 7q31.33 - q-ter. | 123544140 | 158605053 | 35.1 | >10 genes |

*Physical localization and size (Mb) are obtained from UCSC Genome Browser. Copy number changes previously described as copy number variant were excluded. CNN-LOH; copy number neutral loss of heterozygosity, Del; deletion, Dup; duplication, Tri; trisomy, Mono; monosomy, ter.; terminal.*

demonstrating that *KIT*-D816 mutation is significantly associated with Group B ($p<0.05$, $\chi^2$ test). This result suggests that copy number changes are often involved in cases with a *KIT*-D816 mutation in t(8;21) AML.

### Recurrent copy number changes in t(8;21) acute myeloid leukemia samples

Two cases (#34 and #37) had a duplication on chromosome 8 from 8q22.1 to q-terminal including the *MYC* gene; and 2 cases (#13 and #28) had a trisomy/duplication on chromosome 15 with common duplicated region at 15q21.1-15q-terminal (53.7 Mb). Four cases (#14, #34, #43 and #60) had a deletion/monosomy on chromosome 7 with a common deleted region at 7q35 - 7q36.1 (2.1 Mb) including the *CUL1* and *EZH2* genes; and 2 cases (#17 and #34) had a deletion on chromosome 9 with the common deleted region at 9q13 - 9q36.1 (16.2 Mb). Interestingly, a frequent large duplication was found on chromosome 4. Two cases had trisomy 4, and one case had a large region of duplication on chromosome 4 from 4p16.1 to q28.3 (131.1 Mb). All of these amplifications covered the region of the *KIT* gene; and 3 of these cases (#26, #37 and #39) had a *KIT* mutation of either D816Y, D816V or D820G. Amplification of chromosome 4 linked to *KIT* mutations has previously been described in systemic mastocytosis.[21] Thus, the probable increased expression of the mutated form of *KIT* by trisomy 4 or duplication in the region of the gene should give the clone a proliferative advantage.

### Validation of copy number change by fluorescence in situ hybridization (FISH)

To validate some of these copy number changes, we used an interphase FISH approach. Case #34 had a duplication of 8q22.1-8q-terminal (46.6 Mb) including the *MYC* gene and a deletion of 7q31.2-7q-terminal (42.0 Mb). The 8q duplication was confirmed using FISH probes for *MYC* and the centromere of chromosome 8 (*Online Supplementary Figure S2A*). In the same case, deletion of chromosome 7q (q31.2 to q-terminal) was confirmed using FISH probes for 7p telomere and

7q telomere (*Online Supplementary Figure S2B*). Case #28 had a large duplication of chromosome 15 (53.7 Mb). The duplication was confirmed using FISH probes for *SNRPN* and 15q telomere (*Online Supplementary Figure S2C*). These results suggest that abnormalities detected by SNP-chip analysis reflected real alterations in AML cells.

### Chromosomal regions and candidate genes in genomic areas with copy number neutral loss of heterozygosity (CNN-LOH)

Four cases (8%) had CNN-LOH (Table 1 and *Online Supplementary Figure S1*). Case #7 has CNN-LOH at 11p-terminal-11p12 (40.5 Mb) which included the *CDKN1C*, *HRAS*, *WT1* and *LMO2* genes. Case #39 and #41 have CNN-LOH at 6p-terminal - 6p12.3 (46.8 Mb) and at 6p-terminal - 6p21.1 (44.7 Mb), respectively; and the region contained the *PIM1* and *CDKN1A* genes (Table 1 and *Online Supplementary Figure S3*). Case #59 had CNN-LOH at 11q13.2-q-terminal (67.2 Mb). Raghavan *et al.*[15] showed that approximately 20% AML samples had CNN-LOH, and Gondek *et al.*[16] found that 20% of MDS, 23% of MDS-derived AML, and 35% of MDS/MPD patients had CNN-LOH. In additional studies, we found that 32% of normal karyotype AML samples and 15% of t(15;17) APL samples had CNN-LOH.[17,18] CNN-LOH in t(8;21) AML is less frequent than many other types of leukemia.

### Acquired mutation of the PIM1 gene

The protooncogene *PIM1*, which encodes the serine-threonine protein kinase, is located on chromosome 6p, and 2 cases had CNN-LOH in the region. All exons of the *PIM1* gene for these 2 cases were examined for mutations. As shown in Figure 1A, case #39 had a nucleic acid change of G to A at exon 4 of the *PIM1* gene leading to an amino acid change of glutamic acid (E) to lysine (K) at codon 135 (E135K). The amino acid change occurred between the ATP-binding site and serine-threonine kinase domain. The wild-type amino acid is conserved between human, rat, mouse and xenopus. Importantly, the complete remission sample of the same individual showed the wild-type sequence, demonstrating that the nucleic acid change was a disease-specific acquired alteration.

The missense mutation in the *PIM1* gene change produces the recognition site of a restriction enzyme, Hpy188III. A total of 34 t(8;21) AML samples and 40 normal blood DNA samples were examined for this mutation by Hpy188III digestion. The PCR product (178 bp) encompassing the mutation was only digested in case #39 (Figure 1B), but not the DNA from the other AML samples or normal blood DNA (*data not shown*), suggesting it is infrequent in the AML subtype. We also examined all exons of the *PIM1* gene by SSCP using 34 t(8;21) AML samples, but no shifted bands were detected other than exon 4 of case #39. The *PIM1* E135K mutant was also detected in B-cell diffuse large-cell lymphoma;[22] and another mutant (E135Q) was discovered in primary diffuse large B-cell lymphomas.[23] It remains to be clarified whether the E135K mutant is activated constitutively.

### Prognostic significance of genomic change

Overall survival of t(8;21) AML patients of Group A (no genomic abnormality observed by SNP-chip) was significantly better than individuals in Group B (genomic abnormality observed by SNP-chip) (hazard ratio=2.992 [95% confidence interval, 1.247-7.179], $p$=0.01) (Figure 2). The event-free survival of individuals of Group A was also significantly better than those in Group B (hazard ratio=2.360 [95% confidence interval, 1.037-5.372], $p$=0.0347). We also compared the prognosis of individuals with the *KIT*-D816 mutation (6 cases) to those without the alteration (10 cases) in Group B, but found no significant difference (*data not shown*). These results strongly suggest that genomic changes in t(8;21) AML are associated with a poor overall and event-free survival.

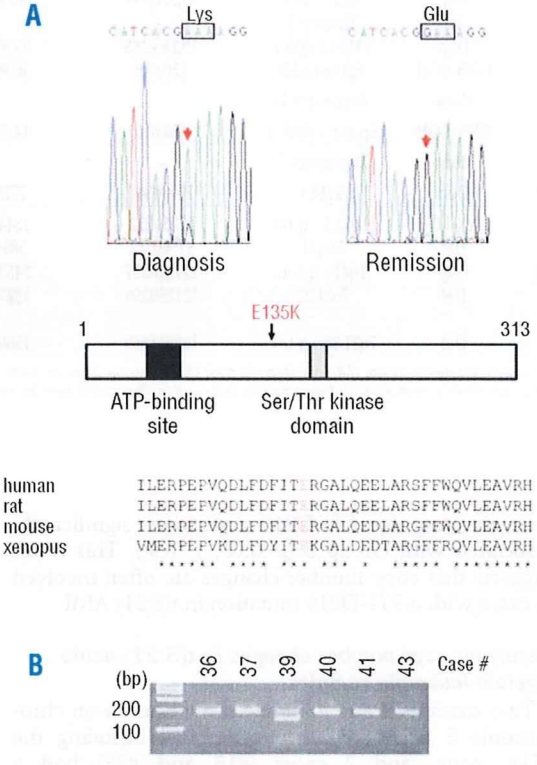


**Figure 1.** Acquired mutation of the *PIM1* gene in case #39. (A) Exon 4 of the *PIM1* gene in case #39 had a missense mutation in the sample at diagnosis but not at remission (top panel). The mutation leads to the amino acid change of glutamic acid (E) to lysine (K) at amino acid 135 (E135K) of PIM1 protein. This mutated amino acid is located between the ATP binding domain and serine-threonine kinase domain of the protein (middle panel). The wild-type amino acid (E) is highly conserved among human, rat, mouse and xenopus (bottom). Note, *identical amino acid. (B) The mutated DNA sequence produced a Hpy188III restriction enzyme recognition sequence. The region was amplified by PCR, digested with Hpy188III, and subjected to agarose gel electrophoresis. The PCR product from only case #39 was digested.

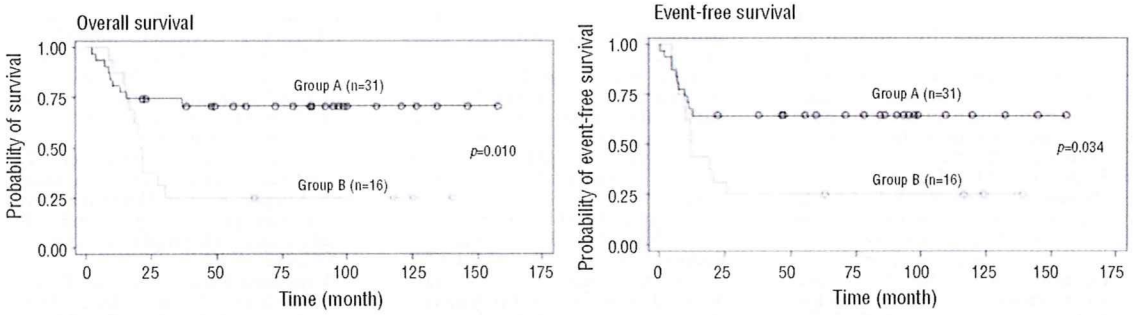


**Figure 2. Comparison of overall survival and event-free survival of t(8;21) acute myeloid leukemia patients either with or without genomic changes. Overall survival (left) and event-free survival (right) were compared between Groups A and B. Black and grey lines indicate Group A (no genomic abnormality by SNP-chip) and Group B (genomic abnormality by SNP-chip), respectively.**

A recent study showed that a *KIT*-D816V mutation is associated with a poor prognosis in t(8;21) AML patients.[9] Also, secondary cytogenetic abnormalities including trisomy of chromosome 8 and 4, deletion/duplication of chromosome 7, as well as deletion of chromosome X and Y in t(8;21) AML have previously been reported to be associated with a poor prognosis.[24] Taken together, these findings indicate that genomic alterations and *KIT*-D816 mutation confer a poor prognosis in t(8;21) AML patients. Further studies in a larger cohort of patients will begin to stratify prognostically the patients in relation to the genomic changes; and new therapeutic targets should be discovered.

## Authorship and Disclosures

TA performed research, analyzed the data and wrote the paper; LS and DL determined mutation of genes; SO, MS, and YN performed SNP-chip analysis and developed CNAG; NK, SD, and JS assisted data analysis; JG and MM performed statistical analysis; VZ and AN performed the methylation analysis; SRM and RS performed FISH analysis; and SL and HPK directed the overall study. TA, LS and SO contributed equally in this work; and SL and HPK are co-last authors.

The authors reported no potential conflicts of interest.

## References


1. Miyamoto T, Weissman IL, Akashi K. AML1/ETO-expressing nonleukemic stem cells in acute myelogenous leukemia with 8;21 chromosomal translocation. Proc Natl Acad Sci USA 2000;97:7521-6.
2. Mori H, Colman SM, Xiao Z, Ford AM, Healy LE, Donaldson C, et al. Chromosome translocations and covert leukemic clones are generated during normal fetal development. Proc Natl Acad Sci USA 2002;99:8242-7.
3. Wiemels JL, Xiao Z, Buffler PA, Maia AT, Ma X, Dicks BM, et al. In utero origin of t(8;21) AML1-ETO translocations in childhood acute myeloid leukemia. Blood 2002;99:3801-5.
4. Rhoades KL, Hetherington CJ, Harakawa N, Yergeau DA, Zhou L, Liu LQ, et al. Analysis of the role of AML1-ETO in leukemogenesis, using an inducible transgenic mouse model. Blood 2000;96:2108-15.
5. Fenske TS, Pengue G, Mathews V, Hanson PT, Hamm SE, Riaz N, et al. Stem cell expression of the AML1/ETO fusion protein induces a myeloproliferative disorder in mice. Proc Natl Acad Sci USA 2004;101:15184-9.
6. Yuan Y, Zhou L, Miyamoto T, Iwasaki H, Harakawa N, Hetherington CJ, et al. AML1-ETO expression is directly involved in the development of acute myeloid leukemia in the presence of additional mutations. Proc Natl Acad Sci USA 2001;98:10398-403.
7. Higuchi M, O'Brien D, Kumaravelu P, Lenny N, Yeoh EJ, Downing JR. Expression of a conditional AML1-ETO oncogene bypasses embryonic lethality and establishes a murine model of human t(8;21) acute myeloid leukemia. Cancer Cell 2002;1:63-74.
8. Care RS, Valk PJ, Goodeve AC, Abu-Duhier FM, Geertsma-Kleinekoort WM, Wilson GA, et al. Incidence and prognosis of c-KIT and FLT3 mutations in core binding factor (CBF) acute myeloid leukaemias. Br J Haematol 2003;121:775-7.
9. Schnittger S, Kohl TM, Haferlach T, Kern W, Hiddemann W, Spiekermann K, et al. KIT-D816 mutations in AML1-ETO-positive AML are associated with impaired event-free and overall survival. Blood 2006;107:1791-9.
10. Schessl C, Rawat VP, Cusan M, Deshpande A, Kohl TM, Rosten PM, et al. The AML1-ETO fusion gene and the FLT3 length mutation collaborate in inducing acute leukemia in mice. J Clin Invest 2005;115:2159-68.
11. Kuchenbauer F, Schnittger S, Look T, Gilliland G, Tenen D, Haferlach T, et al. Identification of additional cytogenetic and molecular genetic abnormalities in acute myeloid leukaemia with t(8;21)/AML1-ETO. Br J Haematol 2006;134:616-9.
12. Nannya Y, Sanada M, Nakazaki K, Hosoya N, Wang L, Hangaishi A, et al. A robust algorithm for copy number detection using high-density oligonucleotide single nucleotide polymorphism genotyping arrays. Cancer Res 2005;65:6071-9.
13. Yamamoto G, Nannya Y, Kato M, Sanada M, Levine RL, Kawamata N, et al. Highly sensitive method for genomewide detection of allelic composition in nonpaired, primary tumor specimens by use of affymetrix single-nucleotide-polymorphism genotyping microarrays. Am J Hum Genet 2007;81:114-26.

14. Kawamata N, Ogawa S, Zimmermann M, Kato M, Sanada M, Hemminki K, et al. Molecular allelokaryotyping of pediatric acute lymphoblastic leukemias by high-resolution single nucleotide polymorphism oligonucleotide genomic microarray. Blood 2008;111:776-84.
15. Raghavan M, Lillington DM, Skoulakis S, Debernardi S, Chaplin T, Foot NJ, et al. Genome-wide single nucleotide polymorphism analysis reveals frequent partial uniparental disomy due to somatic recombination in acute myeloid leukemias. Cancer Res 2005;65:375-8.
16. Gondek LP, Tiu R, O'Keefe CL, Sekeres MA, Theil KS, Maciejewski JP. Chromosomal lesions and uniparental disomy detected by SNP arrays in MDS, MDS/MPD, and MDS-derived AML. Blood 2008; 111: 1534-42.
17. Akagi T, Ogawa S, Dugas M, Kawamata N, Yamamoto G, Nannya Y, et al. Frequent genomic abnormalities in acute myeloid leukemia/myelodysplastic syndrome with normal karyotype. Haematologica 2009; 94:213-23.
18. Akagi T, Shih LY, Kato M, Kawamata N, Yamamoto G, Sanada M, et al. Hidden abnormalities and novel classification of t(15;17) acute promyelocytic leukemia (APL) based on genomic alterations. Blood 2009;113: 1741-8.
19. Downing JR, Head DR, Curcio-Brint AM, Hulshof MG, Motroni TA, Raimondi SC, et al. An AML1/ETO fusion transcript is consistently detected by RNA-based polymerase chain reaction in acute myelogenous leukemia containing the (8;21) (q22;q22) translocation. Blood 1993; 81:2860-5.
20. Shih LY, Liang DC, Huang CF, Chang YT, Lai CL, Lin TH, et al. Cooperating mutations of receptor tyrosine kinases and Ras genes in childhood core-binding factor acute myeloid leukemia and a comparative analysis on paired diagnosis and relapse samples. Leukemia 2008;22: 303-7.
21. Beghini A, Ripamonti CB, Castorina P, Pezzetti L, Doneda L, Cairoli R, et al. Trisomy 4 leading to duplication of a mutated KIT allele in acute myeloid leukemia with mast cell involvement. Cancer Genet Cytogenet 2000;119:26-31.
22. Pasqualucci L, Neumeister P, Goossens T, Nanjangud G, Chaganti RS, Küppers R, et al. Hypermutation of multiple proto-oncogenes in B-cell diffuse large-cell lymphomas. Nature 2001;412:341-6.
23. Montesinos-Rongen M, Van Roost D, Schaller C, Wiestler OD, Deckert M. Primary diffuse large B-cell lymphomas of the central nervous system are targeted by aberrant somatic hypermutation. Blood 2004;103: 1869-75.
24. Marcucci G, Mrózek K, Ruppert AS, Maharry K, Kolitz JE, Moore JO, et al. Prognostic factors and outcome of core binding factor acute myeloid leukemia patients with t(8;21) differ from those of patients with inv(16): a Cancer and Leukemia Group B study. J Clin Oncol 2005;23:5705-17.

ELSEVIER

Experimental Hematology

Experimental Hematology 2009;37:937–946

# Identified hidden genomic changes in mantle cell lymphoma using high-resolution single nucleotide polymorphism genomic array

Norihiko Kawamata[a,*], Seishi Ogawa[b,*], Saskia Gueller[a], Samuel H. Ross[a], Thien Huynh[a], John Chen[a], Andrew Chang[a], Shayan Nabavi-Nouis[a], Nairi Megrabian[a], Reiner Siebert[c], Jose A. Martinez-Climent[d,†], and H. Phillip Koeffler[a,†]

[a]*Hematology/Oncology, Cedars-Sinai Medical Center/UCLA School of Medicine, Los Angeles, Calif., USA;* [b]*Regeneration Medicine of Hematopoiesis, University of Tokyo, School of Medicine, Tokyo, Japan;* [c]*Institute of Human Genetics, University Hospital Schleswig-Holstein, University of Kiel, Kiel, Germany;* [d]*Division of Oncology, Center for Applied Medical Research, University of Navarra, Pamplona, Spain*

(Received 29 September 2008; revised 30 March 2009; accepted 28 April 2009)

***Objective.*** **Mantle cell lymphoma (MCL) is a lymphoma characterized by aberrant activation of *CCND1*/cyclin D1 followed by sequential genetic abnormalities. Genomic abnormalities in MCL have been extensively examined by classical cytogenetics and microarray-based comparative genomic hybridization techniques, pointing out a number of alterations in genomic regions that correlate with the neoplastic phenotype and survival. Recently, single nucleotide polymorphism genomic microarrays (SNP-chip) have been developed and used for analysis of cancer genomics. This technique allows detection of genomic changes with higher resolution, including loss of heterozygosity without changes of gene dosage, so-called acquired uniparental disomy (aUPD).**

***Materials and Methods.*** **We have examined 33 samples of MCL (28 primary MCL and 5 cell lines) using the 250,000 SNP-chip from Affymetrix.**

***Results.*** **Known alterations were confirmed by SNP arrays, including deletion of INK4A/ARF, duplication/amplification of MYC, deletion of ATM, and deletion of TP53. We also identified a duplication/amplification that occurred at 13q involving oncogenic microRNA, miR17-92. We found other genomic abnormalities, including duplication/amplification of cyclin D1, del(1p), del(6q), dup(3q) and dup(18q). Our SNP-chip analysis detected these abnormalities at high resolution, allowing us to narrow the size of the commonly deleted regions, including 1p and 6q. Our SNP-chip analysis detected a number of aUPD sites, including whole chromosome 9 aUPD and 9p aUPD. We also found an MCL case with 19p, leading to homozygous deletion of TNFSF genes.**

***Conclusion.*** **SNP-chip analysis detected in MCL very small genomic gains/losses, as well as aUPDs, which could not be detected by more conventional methods.** © **2009 ISEH - Society for Hematology and Stem Cells. Published by Elsevier Inc.**

Mantle cell lymphoma (MCL) is one of the subtypes of B-cell non-Hodgkin lymphoma derived from the mantle cell [1-3]. This disease develops in elderly male patients predominantly [1-3]. The disease-free and progression-free survival of MCL is worse than many other types of lymphomas, including diffuse large B-cell lymphoma. Although MCL usually responds to initial chemotherapy, the disease often relapses after a short duration of remission. Recently, an antibody (rituximub) targeting CD20 on the B-cell lymphoma cells has often been used with chemotherapy as initial therapy with some improvement in disease-free survival [4,5].

This disease is characterized by chromosomal translocation, t(11;14)(q13;q32), resulting in overexpression of the cyclin D1 gene on 11q23 driven by the enhancer region of immunoglobulin heavy chain (IgH) gene on 14q32 [1-3]. Of interest, transgenic mice mimicking this change develop lymphoid hyperplasia only, suggesting that overexpression of cyclin D1 in lymphoid cells is not sufficient to

*Drs. Kawamata and Ogawa contributed equally to this work as the first authors.

†Drs. Martinez-Climent and Koeffler contributed equally to this work as the last authors.

Offprint requests to: Seishi Ogawa, M.D., Ph.D., Regeneration Medicine of Hematopoiesis, University of Tokyo, 7-3-1 Hongo, Bunkyo-ku, Tokyo 113-8655, Japan; E-mail: sogawa-tky@umin.net

0301-472X/09 $–see front matter. 
doi: 10.1016/j.exphem.2009.04.012

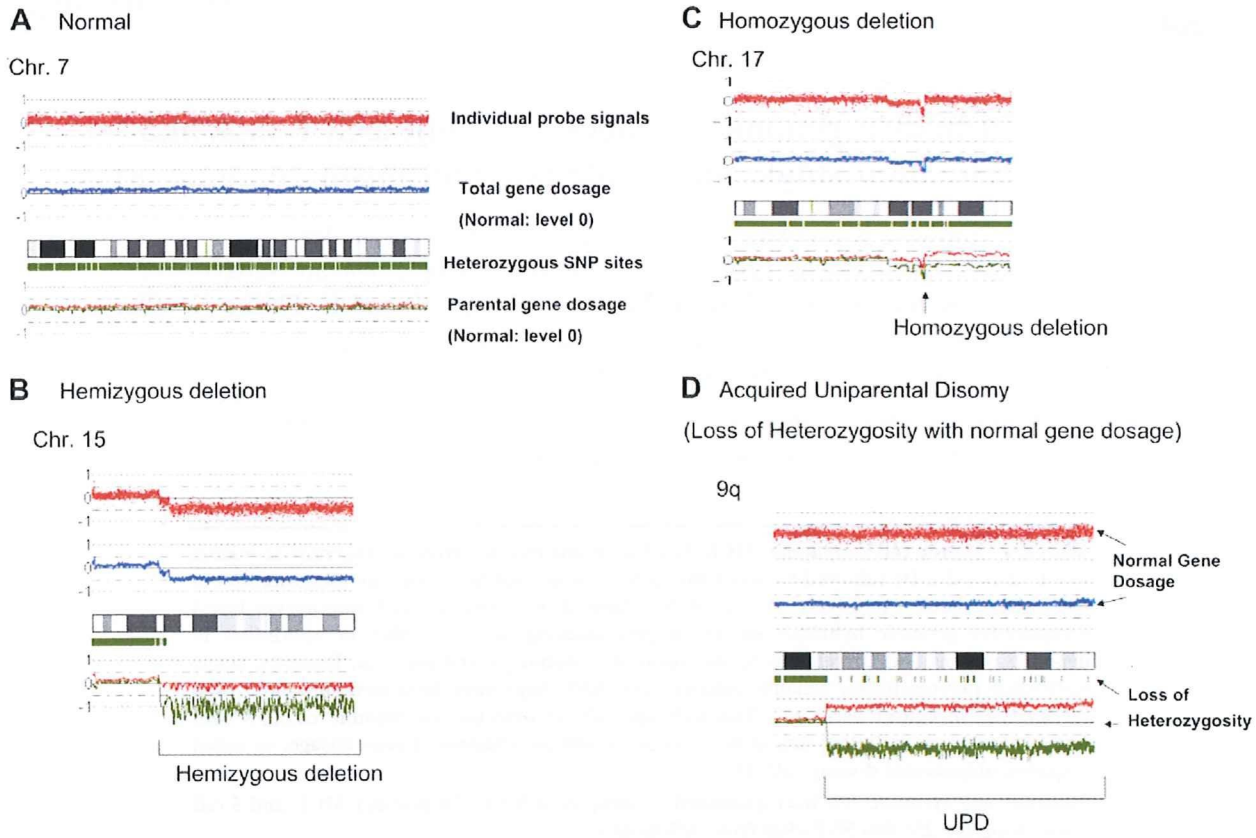


**Figure 1.** Results of single nucleotide polymorphism genomic microarray (SNP-chip) analysis. Representative results and the overview of genomic status of 33 mantle cell lymphoma (MCL) identified by SNP-chip are shown. (**A**) Normal chromosome. Top panel shows individual SNP probe signals; intensity of the signals are almost the same over the entire chromosome. Second panel indicates gene dosage level; gene dosage is normal over the chromosome. Third panel shows heterozygosity SNP sites by green rectangles. Heterozygous SNP site are frequently detected over the chromosome. Fourth panel indicates gene dosage of each parental allele (green or red line); level of each allele is identical over the chromosome. (**B**) Hemizygous deletion. Region of hemizygous deletion is delineated by brackets. (**C**) Homozygous deletion. Arrow indicates a site of homozygous deletion; each parental allele (red or green line) has a deletion at this site. (**D**) Acquired uniparental disomy (aUPD). aUPD is a site that has loss of heterozygosity with normal gene dosage; one of the parental alleles is missing (green line) and the other allele is duplicated (red line). aUPD region is indicated by brackets. This figure is available in color online at www.exphem.org.

cause MCL [6,7]. Additional oncogenic abnormalities must cooperate with cyclin D1 in development of MCL [6,7].

Previous data, including karyotyping and comparative genomic hybridization, showed that MCL has a number of additional genomic abnormalities, including deletion of ATM, p53, and p16INK4/p14ARF [8–11,12]. In addition, expression microarray and protein microarray data revealed dysregulation of apoptosis-associated genes, including Pim1 and MDM2 in this disease [13–16].

However, genomic abnormalities in this disease have not been fully explored. Recently, high-resolution single nucleotide polymorphism genomic microarray (SNP-chip) has been developed and employed in analysis of the cancer genome [17–19]. This novel technique allows us to detect very small gain and/or loss of genomic materials as well as acquired uniparental disomy (aUPD; loss of heterozygosity with neutral gene dosage) [20,21]. We named this new technology molecular allelokaryotyping because SNP-chip is able to detect genomic abnormalities at the molecular level and identify each parental allelic dosage [17,18]. To explore genomic abnormalities in MCL, we employed this new technique and analyzed 33 MCL samples, including 28 primary MCL and 5 MCL cell lines.

## Materials and methods

*Samples and DNA extraction*

We collected MCL cells from 28 newly diagnosed patients with MCL. All cases fulfilled World Health Organization diagnostic criteria for MCL, including overexpression of cyclin D1, presence of t(11;14)(q13; q32) as determined by fluorescence in situ hybridization and/or chromosomal analysis [22]. For case numbers 6505, 22073, 11527, 19358, and 22601, MCL cells were collected from peripheral blood because a large number of the lymphoma cells

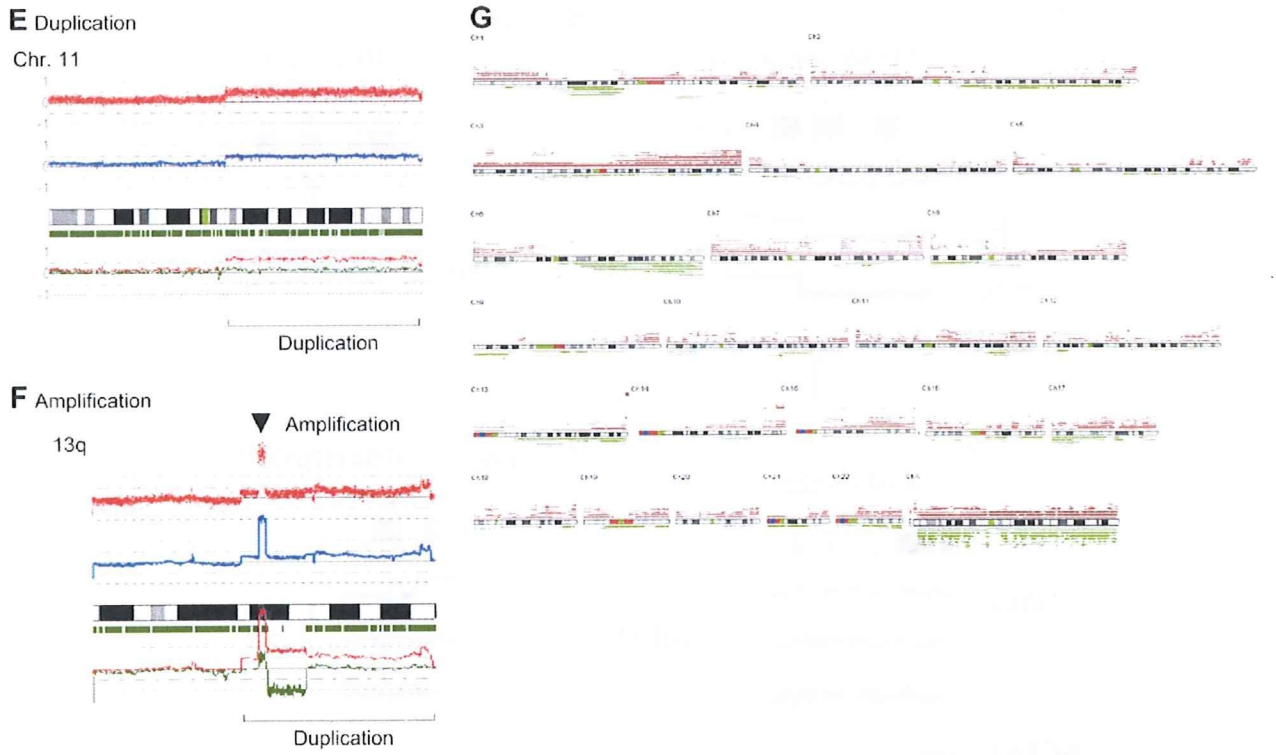


**Figure 1.** *(Continued).* Results of single nucleotide polymorphism genomic microarray (SNP-chip) analysis. Representative results and the overview of genomic status of 33 mantle cell lymphoma (MCL) identified by SNP-chip are shown. (**E**) Duplication. Duplicated region is indicated by a parenthesis. (**F**) Amplification. Arrowhead indicates the sites of high copy number amplification. This case also has duplication at 13q as indicated by the brackets. (**G**) SNP-chip data of 33 cases of MCL. Deleted regions are indicated by green lines under each chromosome panel; and duplications/amplifications are indicated by brown lines above each chromosome panel. This figure is available in color online at www.exphem.org.

were detected in the peripheral blood. Except for these three cases, all MCL cells were collected from lymph-nodes. This study was approved by the institutional review board of the University of Navarra and Cedars-Sinai Medical Center. Patients gave their informed consent per the Declaration of Helsinki. Five MCL cell lines were also studied, i.e., HBL-2, SP-49, REC-1, NCEB-1, and Jeko1. DNA was extracted using Qiagen DNA extraction kit (Qiagen, Valencia, CA, USA) according to manufacturer's protocol.

*SNP-chip analysis*

DNA from the samples was analyzed on Affymetrix GeneChip Human mapping 250K Nsp arrays (Affymetrix Japan, Tokyo, Japan) according to manufacturer's protocol. Microarray data were analyzed for determination of both total and allelic-specific copy numbers using the CNAG program as previously described with minor modifications, where the status of copy numbers as well as UPD at each SNP was inferred using the algorithms based on Hidden Markov Models [20,21].

Allele-specific gene dosage using nonmatched reference samples was measured as follows: SNP-typing on the SNP-chip uses two distinct sets of SNP-specific probes named "A-" and "B-"SNPs at all SNP sites. At each SNP site, perfectly matched probes ($PM_A$s or $PM_B$s) and mismatched probes ($MM_A$s or $MM_B$s) are placed on the chip. For the allele-specific gene-dosage measurement, sums of perfectly matched probes ($PM_A$s or $PM_B$s) for the $i$th SNP site in the tumor and reference samples (ref1, ref2, ref3, . . . , ref$N$),

$$S^{tum}_{A,i}=\sum PM^{tum}_{A,i},\ S^{tum}_{B,i}=\sum PM^{tum}_{B,i} \text{ and}$$
$$S^{refI}_{A,i}=\sum PM^{frefI}_{A,i},\ S^{refI}_{B,i}=\sum PM^{refI}_{B,i},$$
$$(I=1,\ 2,\ 3,\ ,\ N)$$

are compared at each SNP site, according to the concordance of the SNP calls in the tumor sample ($O^{tum}{}_i$), and the SNP calls in a given reference sample ($O^{refI}{}_i$),

$$R^{refI}_{A,i}=S^{tum}_{A,i}/S^{refI}_{A,i}\quad R^{refI}_{B,i}=S^{tum}_{B,i}/S^{refI}_{B,i}\quad (\text{for } O^{tum}_i=O^{refI}_i)$$

and the total CN (copy number) ratio was calculated as follows:

$$\begin{aligned}R^{refI}_{AB,i}&=R^{refI}_{A,i}\ \text{for}\ O^{tum}_i=O^{refI}_i=AA\\&=R^{refI}_{B,i}\ \text{for}\ O^{tum}_i=O^{refI}_i=BB\\&=1/2\ \left(R^{refI}_{a,i}+R^{refI}_{B,i}\right)\ \text{for}\ O^{tum}_i=O^{refI}_i=AB\\&\quad (I=1,\ 2,\ 3,\ \ldots\ldots,\ N)\end{aligned}$$

To obtain adjusted values ($R^{refI}_{AB,i}$, $R^{refI}_{A,i}$ and $R^{refI}_{B,i}$), calculated signals were compensated as reported previously [20].